

Lawrence Berkeley National Laboratory

LBL Publications

Title

Mineral and fluid transformation of hydraulically fractured shale: case study of Caney Shale in Southern Oklahoma

Permalink

<https://escholarship.org/uc/item/92h050nx>

Journal

Geomechanics and Geophysics for Geo-Energy and Geo-Resources, 10(1)

ISSN

2363-8419

Authors

Awejori, Gabriel A
Dong, Wenming
Doughty, Christine
[et al.](#)

Publication Date

2024-12-01

DOI

10.1007/s40948-024-00835-0

Copyright Information

This work is made available under the terms of a Creative Commons Attribution-NonCommercial License, available at <https://creativecommons.org/licenses/by-nc/4.0/>

Peer reviewed

Mineral and Fluid Transformation of Hydraulically Fractured Shale: Case Study of Caney Shale in Southern Oklahoma

Authors: Gabriel A. Awejori^a, Wenming Dong^b, Christine Doughty^b, Nicolas Spycher^b, Mileva Radonjic^{a*}

^a*Hydraulic Barrier Material and Geomimicry Laboratory, School of Chemical Engineering, Oklahoma State University, 420 Engineering North, Stillwater, OK 74078, USA*

^b*Energy Geosciences Division, Lawrence Berkeley National Laboratory, 1 Cyclotron Road, Berkeley, CA 94720, USA*

**Corresponding author: mileva.radonjic@okstate.edu*

Abstract

This study explores the geochemical reactions that can cause permeability loss in hydraulically fractured reservoirs. The experiments involved the reaction of powdered-rock samples with produced brines in batch reactor system at temperature of 95°C and atmospheric pressure for 7-days and 30-days respectively. Results show changes in mineralogy and chemistry of rock and fluid samples respectively, therefore confirming chemical reactions between the two during the experiments. The mineralogical changes of the rock included decreases of pyrite and feldspar content, whilst carbonate and illite content showed an initial stability and increase respectively before decreasing. Results from analyses of post-reaction fluids generally corroborate the results obtained from mineralogical analyses. Integrating the results obtained from both rocks and fluids reveal a complex trend of reactions between rock and fluid samples which is summarized as follows. Dissolution of pyrite by oxygenated fluid causes transient and localized acidity which triggers the dissolution of feldspar, carbonates, and other minerals susceptible to dissolution under acidic conditions. The dissolution of minerals releases high concentrations of ions, some of which subsequently precipitate secondary minerals. On the field scale, the formation of secondary minerals in the pores and flow paths of hydrocarbons can cause significant reduction in the permeability of the reservoir, which will culminate in rapid productivity decline.

This study provides an understanding of the geochemical rock-fluid reactions that impact long term permeability of shale reservoirs.

Statements and Declarations

Funding

This study was funded by the US Department of Energy (DOE), Office of Fossil Energy, Award DE-FE0031776.

Competing Interest

The authors have no competing interests as defined by Springer, or other interests that might be perceived to influence the results and/or discussion reported in this paper.

Article Highlights

- Dissolved oxygen in fluids is crucial for initiating geochemical rock-fluid reactions.
- The breakdown and oxidation of sulfides create transient and localized acidity to trigger the dissolution of minerals in reservoir rock.

- Post-hydraulic fracturing reactions can induce ductile properties in an originally brittle reservoir rock and aid fracture healing.

Key Words: Shale, Unconventional Reservoir, Produced Brine, Hydraulic Fracturing, Mineralogy

1.0 Introduction

Increasing demand for energy has accelerated the growth of the unconventional hydrocarbon industry following the United States (US) shale boom in the early part of the last decade (Wang and Krupnick 2013). According to the US Energy Information Agency (US EIA), unconventional oil and gas will contribute the largest share of the total energy mix in the United States for the most part of the 21st century. The US currently has an estimated reserve of 6 trillion barrels of oil and 495 trillion cubic feet of gas in unconventional reservoirs (Farrokhrouz et al. 2022). Some significant and established unconventional shales currently under exploitation include Barnett, Bakken, Marcellus, Eagle Ford, and Woodford shales. To increase the reserves of oil and gas in unconventional shale reservoirs, petroleum companies continue to invest in exploration projects. One of the emerging shale plays in the midcontinent of the United States is the Caney Shale of South-Central Oklahoma Oil Province (SCOOP).

Though unconventional shale reservoirs are replete with substantial hydrocarbons, these reservoirs are complex and challenging to exploit. Shales are characterized by complex and heterogeneous mineralogy. They also exhibit ultra-low permeability which renders most hydrocarbons immobile. According to the US EIA, 2013 report on recovery from shale oil and shale gas, the ultimate recovery from unconventional reservoirs was less than 25% for natural gas and less than 5% for oil. In a recent publication, Mukhina et al. (2021) stated that the ultimate recovery from shale reservoirs is approximately 10% of initial hydrocarbon in place. More research is currently being undertaken aimed at improving the recovery from unconventional hydrocarbon reservoirs.

Horizontal drilling and hydraulic fracturing are the main technologies employed in developing unconventional reservoirs (Bennour et al. 2015). The objective is to stimulate the reservoir to create fracture networks that increase the permeability of the reservoir. These fracture networks subsequently act as pathways for hydrocarbon migration from reservoir to wellbore (Zeng et al. 2015). Hydraulic fracturing is an expensive operation, yet sometimes the permeability increases achieved from fracturing operations are short lived due to fracture closures over time, causing rapid decline in production (Alfarge et al. 2019). The cause of fracture closure remains a source of debate among researchers though both sides believe fracture closures are caused by a combination of geochemical rock-fluid reactions and high confining pressures in the subsurface. Whilst one group of researchers propose geo-mechanical stresses as the predominant precursor factor to fracture closure (Aslannezhad et al. 2021; Awan et al. 2020, 2021; Bedrikovetsky et al. 2012; Katende et al. 2021, 2023; Keshavarz et al. 2014), others aver that geochemical rock-fluid interaction is the central force in the closure of generated hydraulic fractures (Awejori et al. 2022; Cheng et al., 2021a, 2021b; Gundogar et al. 2021; Wang et al. 2011; Weaver and Rickman 2010). This research supports the latter perspective.

During hydraulic fracturing, fluids are injected under high pressures into the reservoir formation to cause failure of rock thus generating fractures. When fracturing fluids contact the reservoir formation, the resulting chemical disequilibrium sets up chemical reactions between the fluids and rock minerals. These reactions generally occur along the face of the newly created fractures but extend into the matrix over time

(Harrison et al. 2017; Vankeuren et al. 2017; Wilke et al. 2015). In the long-term, geochemical reactions and their products subject the shale formation to adverse petrophysical changes, one of which is permeability loss and consequently hydrocarbon production decline. Following the inception of the US shale boom, there have been several studies to understand the dynamics of production performance from hydraulically fractured reservoirs. Most of these studies have focused on rock-fluid interactions and their impact on formation properties and water chemistry (Barbot et al. 2013; Cai et al. 2018; Cai and Li 2016; Carpenter et al., 2023; Cheng et al. 2017; Tasker et al. 2016; Zeng et al. 2020). This research investigates changes in mineralogy and solution chemistry resulting from the interaction of Caney shale with produced fluids, using laboratory experiments, with the goal to understand geochemical rock-fluid interaction in the subsurface. In these experiments, Caney Shale rock powders were reacted in batches with produced brines from the same formation. The geochemical changes of the rock as well as changes in fluid chemistry were studied in an integrated manner to provide a comprehensive understanding of long-term reaction processes in hydraulically fractured shale reservoirs.

2.0 Literature Review

2.1 Complex Reaction Paths in Shale

‘Unconventional shale reservoir’ has become the generic term to describe argillaceous hydrocarbon-rich formations. These formations are characterized by ultralow permeability. Rock particles in these formations are smaller in size, with critical rock-fluid interactions mostly taking place at the micro and nanoscales (Du et al., 2017, 2020; Zhang et al., 2023). Depositional environments for these formations vary but most are of marine origin (Zou et al. 2013). Due to their depositional environments and high clay content, shales adsorb high concentrations of halogens, alkali earth metals, heavy metals as well as radionuclides. For this reason, the evolution of geochemical rock-fluid interactions between shale formations and hydraulic fracturing fluids varies widely, with major implications for the petrophysical properties of the formation as well as environmental concerns due to elevated concentrations of elements in produced waters (Jew et al. 2022).

Considering the complexity of shales, the type and products of geochemical reactions are sensitive to the composition of hydraulic fracturing fluids. This includes the types and quantity of additives as well as the initial pH of the fluids injected. The pH and amount of dissolved oxygen in hydraulic fracturing fluids have a direct impact on mineral dissolution in the formation and release of ions required for precipitation of new minerals. The initial pH of fluids determines the levels of carbonate dissolution, consequently, the amount of precipitation of minerals like strontianite (SrCO_3) that need carbonate to precipitate (Mavromatis et al., 2017). The presence of oxidants may enhance the dissolution of pyrite, which releases sulfates. The presence of sulfates from the oxidation of sulfide minerals such as pyrite promotes precipitation of celestite (SrSO_4), gypsum (CaSO_4) and other sulfate minerals (Czerewko and Cripps, 2023; Osselin et al., 2019). The breakdown of shale minerals and precipitation of new minerals, especially within the fracture network, adversely impact permeability, thus the extent of formation damage. The heterogeneity of shales also ensures that dissolution and precipitation reactions are not uniform within the reservoir. Thus, geochemical reactions between shales and hydraulic fracturing fluids are typically complex (Harrison, et al. 2017; Li et al. 2002).

2.2 Hydraulic Fracturing and Imbibition

The hydraulic fracturing process entails five stages, which involves the injection of large volumes of liquid into the subsurface formations to generate a fracture network. These stages include 1) injection of pad fluid, 2) injection of proppant slurry fluid, 3) injection of flush fluid, 4) a shut-in period and finally 5) fluid flowback. However, it has been reported that more than 50% of fluids are not recovered during flowback (Alkough and Wattenbarger 2013; Bo et al. 2023). Fluids retained in the formation are believed to largely reside within three areas of the formation. These include the newly created fractures, secondary and reactivated natural fractures, and to the largest extent, within the rock matrix due to imbibition (Fan et al. 2010; Ghanbari et al. 2013; Makhanov et al. 2014; Wang and Leung 2015; Zhong and Leung 2020). Additionally, the rate of imbibition has been observed to be proportional to the amount of oxidation of the injected fluid (You et al., 2018).

Imbibition is the displacement of immiscible fluids between the exterior and interior segments of a formation matrix and this phenomenon is a common occurrence during hydraulic fracturing. The hydraulic fracturing fluid therefore serves as the fluid in the exterior of the matrix whilst the interior fluids include formation brine, oil, and gas. Capillary forces acting within the matrix have been identified as responsible for imbibition of fracturing fluids into the formation matrix (Farhadzadeh and Nick 2023; Kasiri and Bashiri 2011; Siddiqui et al. 2019). Though this statement is true for sandstone formations, the dynamics are relatively different in shale formations where osmosis diffusion plays significant roles in imbibition (Zhou et al. 2016).

Osmosis diffusion occurs when water molecules are moved from a region of lower solution concentration (higher water content) to a region of higher solution concentration (lower water content) through a semi-permeable membrane. The importance of a semi-permeable membrane is that it permits the transmission of certain molecules whilst other molecules are inhibited from crossing due to their electrical properties and their size (Tuwiner et al. 1962). In shale formations with high clay contents, the clay minerals in the formation act as the semi-permeable membrane due to their salt exclusionary character induced by structure and electrical restriction (Fritz 1986). The net negative charges induced on the surface of clay attract cations whilst anions are repelled, therefore limiting the movement of the cations to the surface of the clays (Stumm and Morgan 2012). Water, however, can be transmitted across the clay structure. This mechanism has been known in the petroleum industry and typically occurs during drilling and water flooding operations (Bol et al. 1994; Fakcharoenphol et al. 2014; Lu et al. 2012). The occurrence of this mode of imbibition has been identified in hydraulic fracturing operations and observed to be one of the major causes of water retention by the formation matrix.

3.0 Materials and Methodology

3.1 Materials

Samples used in this study were prepared from rock samples collected from a well drilled in the Caney Shale. This well is located within the Ardmore Basin of Southern Oklahoma, one of the basins where the Caney Shale is present (Paronish et al. 2020). The well was drilled across five (5) zones designated as reservoir and ductile formations within the Caney Shale (Radonjic et al. 2020; Wang et al. 2021). The samples were collected as core-plugs at selected depths of each zone, mainly from a 4-inch recovered cored rock. For the purposes of this article, the samples are designated as R1 (Reservoir 1), D1 (Ductile 1), R2 (Reservoir 2), D2 (Ductile 2) and R3 (Reservoir 3) respectively as shown in Fig. 1.

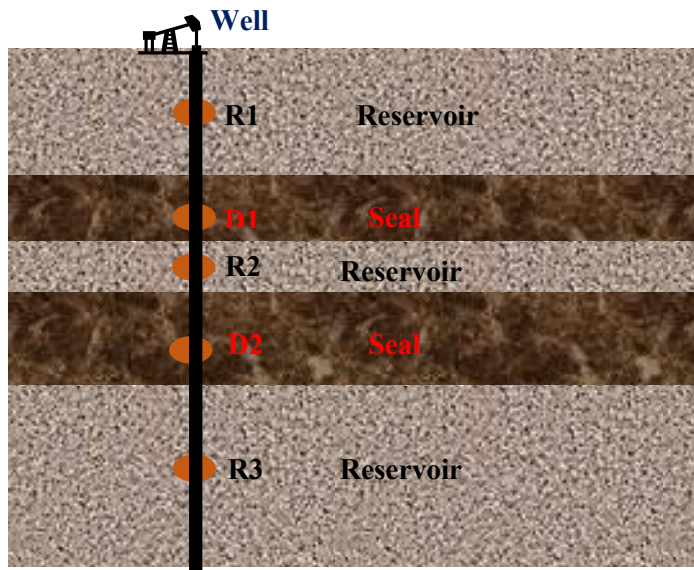


Fig. 1: Schematic showing the sampling locations in Caney Shale according to designated zones.

Fluid used for these set of experiments is produced brine from the field in which the well is drilled, whilst deionized (DI) water is used as a control fluid. The produced brine was recovered after the reservoir had been hydraulically fractured and put into production. This fluid is therefore a hybrid of formation fluid and hydraulic fracturing fluid that has reacted with reservoir rocks. Produced brine is used in experiments as collected from the field, without any extra treatments. At the onset of experiments, the pH of the fluid was circum-neutral (approximately 7). This ensures that this study replicates the conditions in the deeper portions of the reservoir away from wellbore. Fig. 2 is an SEM micrograph of Caney Shale showing the mineralogical composition and microstructure of the rock.

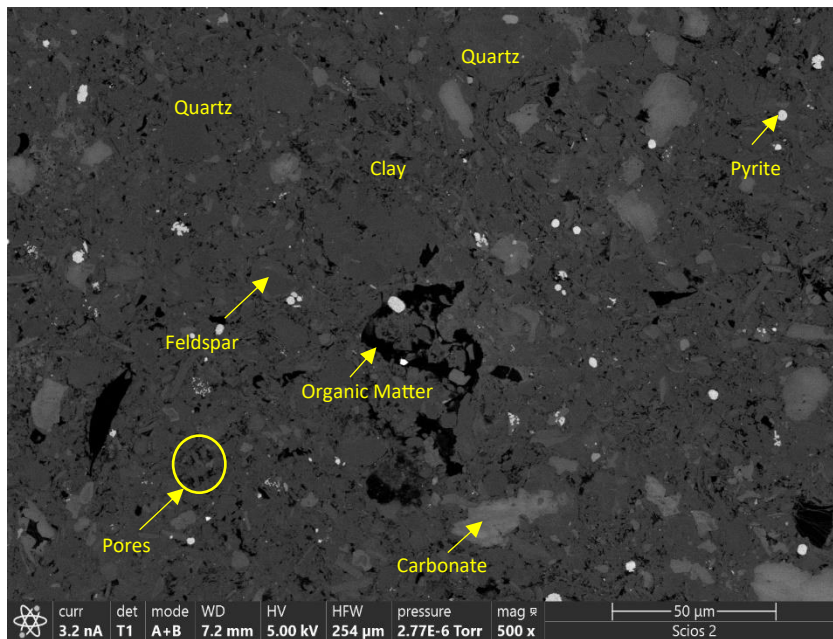


Fig. 2: SEM micrographs showing the mineralogical composition and microstructural configuration of Shale sample. The minerals present include quartz, feldspar, carbonates, and clays.

3.2 Experimental Design and Constraints

The experimental method adopted for this study is the batch reactor experiment, where samples are prepared and put through experimental conditions in batches such that comparable samples are exposed to the same conditions at a given time. For this study, batch experiments were run at reservoir temperature conditions of the Caney Shale (95 °C) and atmospheric pressure. Because the effect of temperature on geochemical reactions is expected to be significantly greater than that of pressure at reservoir conditions (~150 to 450 bar), it is therefore envisaged that reactions during the experiments, approximate reactions between rocks and fluids in the reservoir. The experimental design did not allow the regulation of pressure and therefore the impact of pressure was not evaluated in this study, though results from this study are meant to serve as a basis for studies that will be undertaken in controlled-pressure environments. The reaction times for experiments were 7 days and 30 days .

The bottles used in these experiments are pyrex media storage bottles which have a volume of 250mL and tight seals with the ability to withstand dry temperatures up to 180°C (356°F). Samples were mixed in the bottles and put in heat resistant rectangular containers which were then placed in an oven for the duration of the experiments. The temperature of the oven was monitored daily to ensure there were no fluctuations occurring.

In designing this set of experiments, cognizance was taken of the fact that protocols of hydraulic fracturing treatments include shut-in periods where wells are shut-in for several days to weeks following hydraulic fracturing operations. During this period, the injected fluids are imbibed into the formation and react with both formation fluid and formation rock due to the disequilibrium created. These reactions can cause permeability enhancement or permeability damage. Another important feature of this experiment is the fact that it is designed to mimic long-term reactions in deeper parts of reservoir where the initial acidization of the formation is neutralized.

3.3 Sample Preparation

Samples for experiments were first cored at designated depths from the main rock-core as plugs and subsequently broken into pieces before they were ground with a Spex Ball Mill. The ground powders were then micronized to further reduce the particle sizes using a McCrone Micronizer. Ground powders particle sizes were typically below 100µm with average particle sizes of less than 50µm. This process helps to expose more surface area of the rock during reaction with fluids. The initial liquid to solid ratio used for experiments was 150mL of liquid to 1g of rock powder. During sampling, the fluids were separated from powders by decanting the fluid into empty Pyrex bottles and then filtering 30mL through a 0.22µm filter into glass vials. The sampling of fluids for each reaction vessel lasted approximately three (3) minutes. The remaining rock powders in the bottles were dried, collected, and stored for subsequent examination whilst fluid samples were stored in sealed glass vials in a refrigerator waiting further analyses. To undertake fluid analyses, fluids were taken out of the refrigerator and a syringe was used to collect about 10 ml of fluid, which was again filtered through a 0.22µm filter attached to bottom of the syringe. Sampling during this period lasted approximately two (2) minutes when samples were exposed to atmospheric oxygen.

3.4 Analytical Methods

In evaluating the changes that occur in both original rock powder and fluid samples during the period of reaction, several analytical methods and techniques were used. These include X-ray Diffraction (XRD),

Scanning Electron Microscopy/Energy Dispersive Spectroscopy (SEM/EDS) and Inductively Coupled Plasma Mass Spectroscopy (ICP-MS).

For rock samples, XRD analyses were used to determine the mineralogical contents of samples before and after reaction with produced brines. The Bruker D8 Advanced X-ray Diffractometer with a Lynxeye detector was employed to carry out the XRD measurements of samples. Scanning was run from 5 to 80 degrees 2-theta angles with a step of 0.01-degree and dwell time of 0.5 seconds. Once completed, XRD data were transferred to another computer where the BRUKER's Diffraction software was used to undertake a semi-quantitative evaluation of samples. SEM was conducted on samples using the ThermoFisher FEI Scios2 Dual Beam Scanning Electron Microscope, in both secondary electron mode and in backscattered electron mode. EDS measurements were conducted with a Bruker EDS X-ray microanalysis system which is linked with the ThermoFisher FEI Scios2 Dual Beam Scanning Electron Microscope. The major EDS measurements included point analysis and spot analysis. In taking these point and spot analyses, one point was often taken to capture the substrate on which samples were placed in order to ascertain elemental composition of substrate and identify its associated peak relative to the peaks due to samples.

The concentrations of elements in aqueous samples were evaluated simultaneously using an advanced Agilent 8900 triple quadrupole inductively coupled plasma mass spectrometry system (Agilent 8900 QQQ ICP-MS, Agilent Technologies). The instrument settings and analytical methods are similar to those reported by Belkouteb et al. (2023) and Agilent application notes (Agilent, 4th Edition). All the samples were prepared/diluted using 2% (v/v) ultrapure nitric acid in Milli-Q water (18.2 mΩ-cm) with analyses undertaken under a rigorous quality assurance (QA) and quality control (QC) protocol. The pH measurements were made with an Oakton pH 150 meter with the pH of each fluid measured three times and averaged.

3.5 Modelling Methodology

The reaction of Caney Shale with deionized (DI) water and produced brine (PB) was simulated using the TOUGHREACT v4.13 simulator (Sonnenthal et al. 2021; Xu et al. 2011), together with the Thermodynamic database (Blanc et al. 2012) and equation of state module EOS3 (Pruess et al. 1999). "Batch" simulations (no flow) were set up to represent the reaction bottles, including the effects of the headspace above the sample and the drawing of the atmosphere into the bottles during sampling. A series of simulations were performed to assess a range of oxidizing conditions by varying the O₂ concentration in the atmosphere drawn into the reaction bottle during sampling, to get the best match with the experimental data. Other parameters adjusted to best match experimental results included the relative proportions of the various carbonate minerals (calcite, dolomite, and ankerite) in the simulated sample, whilst keeping the total content of carbonate minerals analyzed by XRD unchanged, and mineral reactive surface areas. The latter were (loosely) calibrated using the data from experiments with DI water (most reactive), then kept at the same calibrated values to model experiments with produced brine (Graphs of results of experiments with DI water is shown in Appendix B). The simulations considered aqueous speciation, mineral dissolution, and precipitation under kinetic constraints (using primarily data from Palandri and Kharaka (2004), together with Smith and Carroll (2016) for chlorite, Yang and Steefel (2008) for kaolinite), and cation exchange using data from Appelo and Postma (2005).

The mineralogy of the shale used in the simulations was evaluated by XRD analyses of the reacted samples (see Section 4.1), coupled with geochemical modelling to assign specific clay minerals (from the thermodynamic database) to the unspecific “illite/smectite” amounts reported from XRD analyses. The reported “albite” was modeled as a low-Ca (An10) plagioclase, using data from Arnorsson and Stefansson (1999) and adjusted for consistency with the Thermoddem database. Additionally, trace amounts (~0.5%) of chlorite, K-feldspar, and organic carbon (modeled as elemental C) were presumed to be present in the reacted shale given that these have been reported to be present in Caney Shale (e.g., Grieser et al. 2007). Specific phases chosen for the modelling are shown in Table 1. The thermodynamic data for ankerite were retrieved from Holland and Powell (1998) since these are not available in the Thermoddem database. The shale minerals shown in Table 1 were determined to be at or near equilibrium with the formation water at 95°C.

Table 1: Solid phases considered in geochemical modelling.

<i>Shale Minerals</i>	
K-feldspar (Microcline)	Illite(Mg)
Albite (Ab90An10-low)	Calcite
Montmorillonite(MgMg)	Dolomite
Ankerite	Pyrite
Chlorite(Cca-2)	C(element)
<i>Potential Secondary Minerals</i>	
Gibbsite Boehmite Ferrihydrite(2L) Chalcedony	
Siderite	
Kaolinite	

ICPMS analyses of metals, data from industry (FracFocus) and other assumptions as shown on Table 2 were used to estimate the simulated composition of the produced brine.

Table 2 Composition of produced brine used in the simulations.

Species	Produced Fluid		
	Initial Values		Source/Assumption
	25°C	95°C	
pH	7.13	6.25	Measured
	ppm	ppm	
Cl	23941	23946	Computed from charge balance
SO ₄	7.7	7.7	Computed assuming barite equilibrium at 25°C
HCO ₃	9	1	Computed assuming atm. CO ₂ equilibrium
Si	22.2	22.2	ICPMS data equilibrated with rock fm. minerals at 95°C
Al	0.107	0.107	ICPMS data equilibrated with rock fm. minerals at 95°C
Ca	495	495	ICPMS data equilibrated with rock fm. minerals at 95°C
Mg	70.2	70.2	ICPMS data equilibrated with rock fm. minerals at 95°C
Fe	6.5	6.5	ICPMS data equilibrated with rock fm. minerals at 95°C

K	74.4	74.4	ICPMS data equilibrated with rock fm. minerals at 95°C
Na	14750	14750	ICPMS data equilibrated with rock fm. minerals at 95°C
B	30.4	30.4	ICPMS data equilibrated with rock fm. minerals at 95°C
Sr	64.3	64.3	ICPMS data equilibrated with rock fm. minerals at 95°C
Ba	8.4	8.4	ICPMS data equilibrated with rock fm. minerals at 95°C
log (FO ₂)	-0.7	-0.7	Atmospheric values at 25°C, then computed
log (FCO ₂)	-3.4	-3.4	Atmospheric values at 25°C, then computed
TDS	39478	39475	

4.0 Results

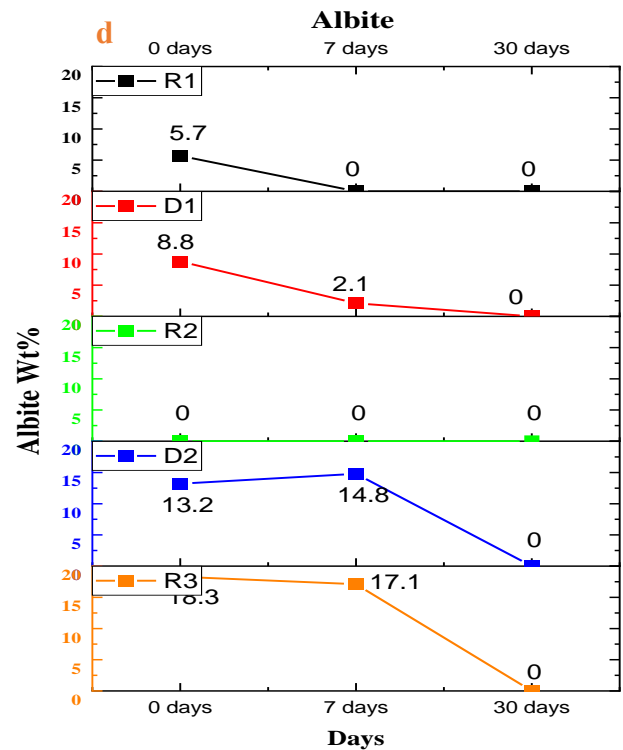
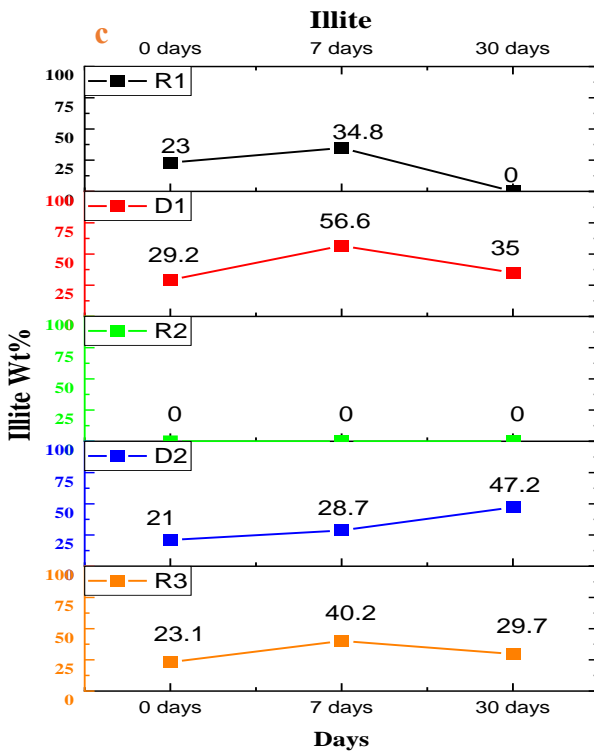
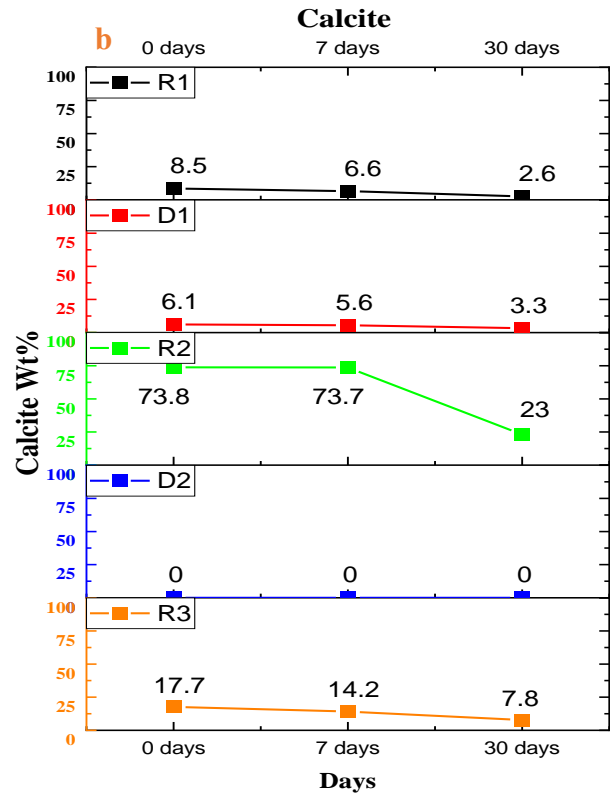
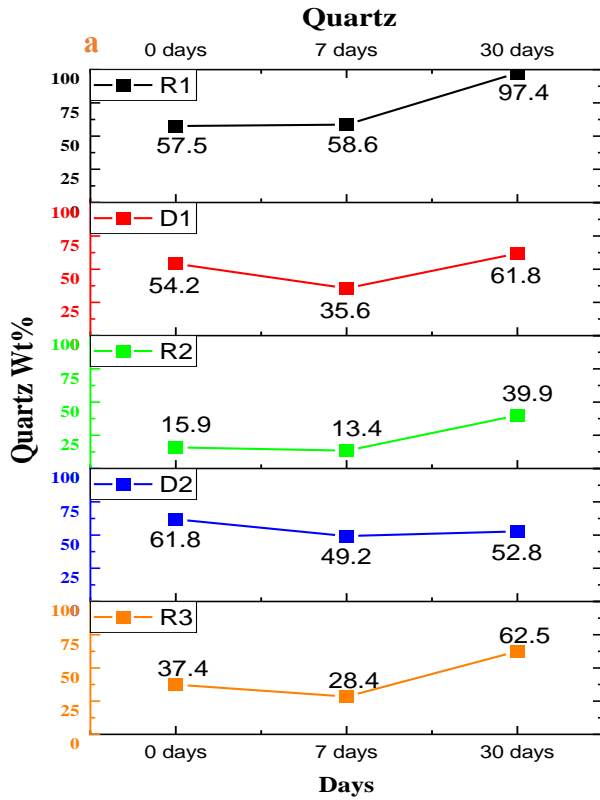
4.1 Mineralogical Composition

The mineralogy of samples show consistency in the type of minerals present but the percentage weight of individual minerals in each sample varies. Minerals identified in the shale samples generally include quartz, illite, albite, calcite, dolomite, pyrite, and traces of other minerals. Reaction with produced brines caused mineralogical changes in the samples as seen in Figure 3 and Appendix A. In general, pyrite and feldspar dissolution were common to all samples following reaction with produced brines. Carbonates were less affected in this experiment, which can be attributed to the circumneutral pH and high Ca concentrations of the reacting fluid. This is a significant change from previous experiments where reaction fluids were acidized or synthesized to represent fracturing fluids with moderate levels of carbonates concentrations (Awejori et al. 2022; Bratcher et al. 2021; Herz-Thyhsen et al. 2019; Jew et al. 2017).

Compared to previous experiments (Awejori et al. 2021, 2022), the mineralogical changes in this experiment were much slower and subtle, which would be expected given that the reacting fluid is a produced brine, thus a fluid that has reacted (at least to some extent) with the shale formation. Based on previous experimental and modelling work (Awejori et al. 2022), reactions in this experiment are believed to proceed in the following order. Dissolution of pyrite is initiated by dissolved oxygen in the reacting fluid, which leads to the generation of transient and localized acidity by the oxidation of the sulfide in pyrite to sulfuric acid. Carbonate minerals proximal to pyrite therefore dissolve in response to the generated acidity, which tends to buffer the pH of the reactant fluid. Feldspar and clay minerals also dissolve. The graphs on Fig. 3 suggest that the amount of feldspar (albite) decline, in many cases corresponding to an increase in illite content. The possible correlation between feldspar decreases and illite increase would suggest that feldspar alters to illite. However, the quartz amounts vary more than expected for this mostly unreactive mineral at low temperatures, suggesting that natural and/or analytical variability cannot be ruled out and could mask small changes in mineral amounts due to dissolution and precipitation. The formation of salts (halite and potassium-based salts) was observed after 7-days of reaction however these minerals were not detected in the 30-days experiments. These are believed to be artifacts and not the products of rock-fluid reactions.

In summary, static batch experiments with produced brines show mineralogical changes that potentially may have significant implications. An increased illite content could enhance the ductile properties to the rock, especially along the fracture-face and near-fracture rock matrix. This could enhance fracture closure under dynamic geo-stress regimes in the subsurface. Increased illite amounts coupled with latter stage decrease of these amounts also indicate the possibility of illite breakdown and clay fines migration in the

formation over the long term. This is often detrimental to permeability of fractures as reported by many researchers.



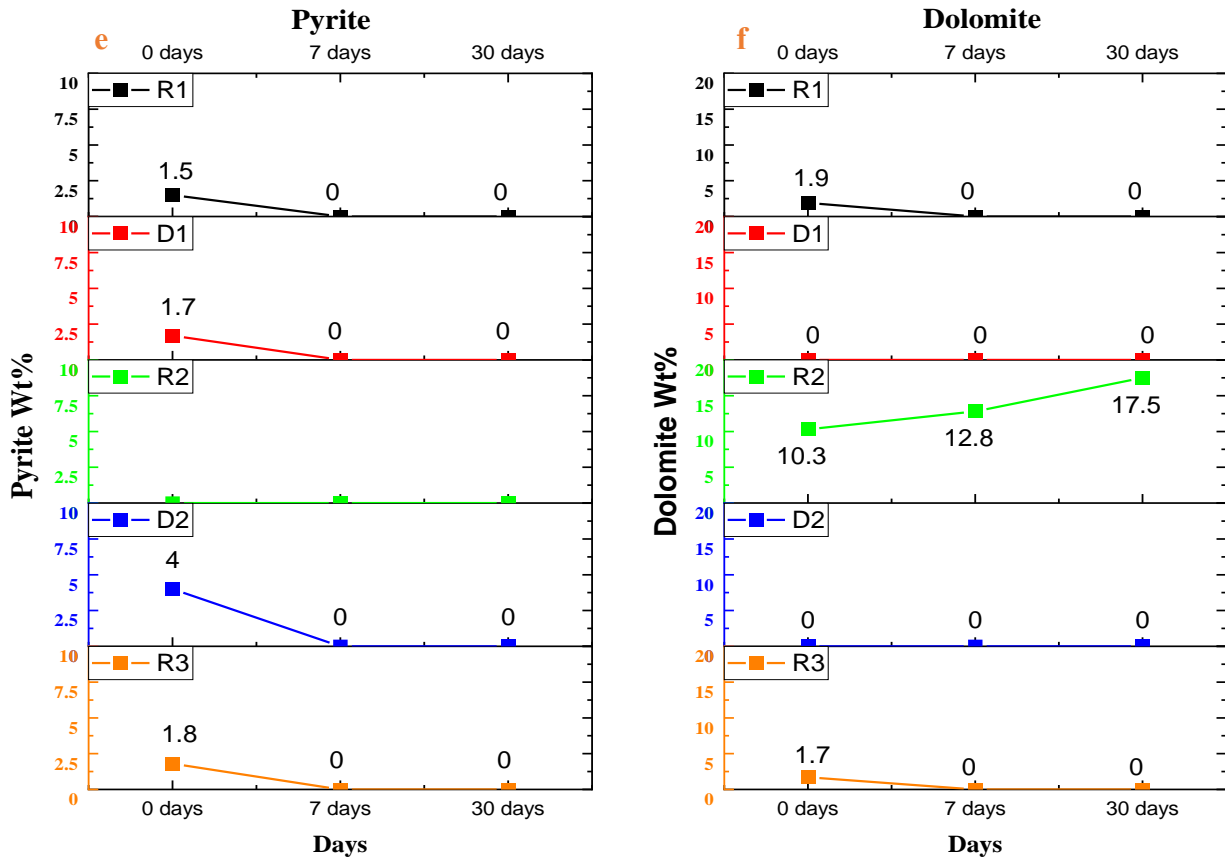


Fig. 3: Changes in mineral (a. Quartz b. Calcite c. Illite d. Albite e. Pyrite f. Dolomite) contents (weight %) in samples from initial composition and after reaction with produced fluids for 7-days and 30-days respectively. Significant shifts are observed for most minerals after reactions.

4.2 Elemental Compositional Changes

Energy Dispersive spectroscopy (EDS) measurements were taken and compared with mineralogical results to ascertain chemical level changes occasioned by reactions between rocks and produced brines. Spot EDS analyses (Figure 4) showed initial samples having high elemental counts with oxygen, silicon, aluminum, and calcium substantiating the relatively high amounts of quartz, illite and carbonate contents. These elemental concentrations are significantly reduced in reacted samples which confirms the breakdown of minerals. Reacted samples also exhibit traces of barium and titanium which were not visible in unreacted samples. This could be due to precipitation of new minerals which allow EDS analyses to capture these elements.

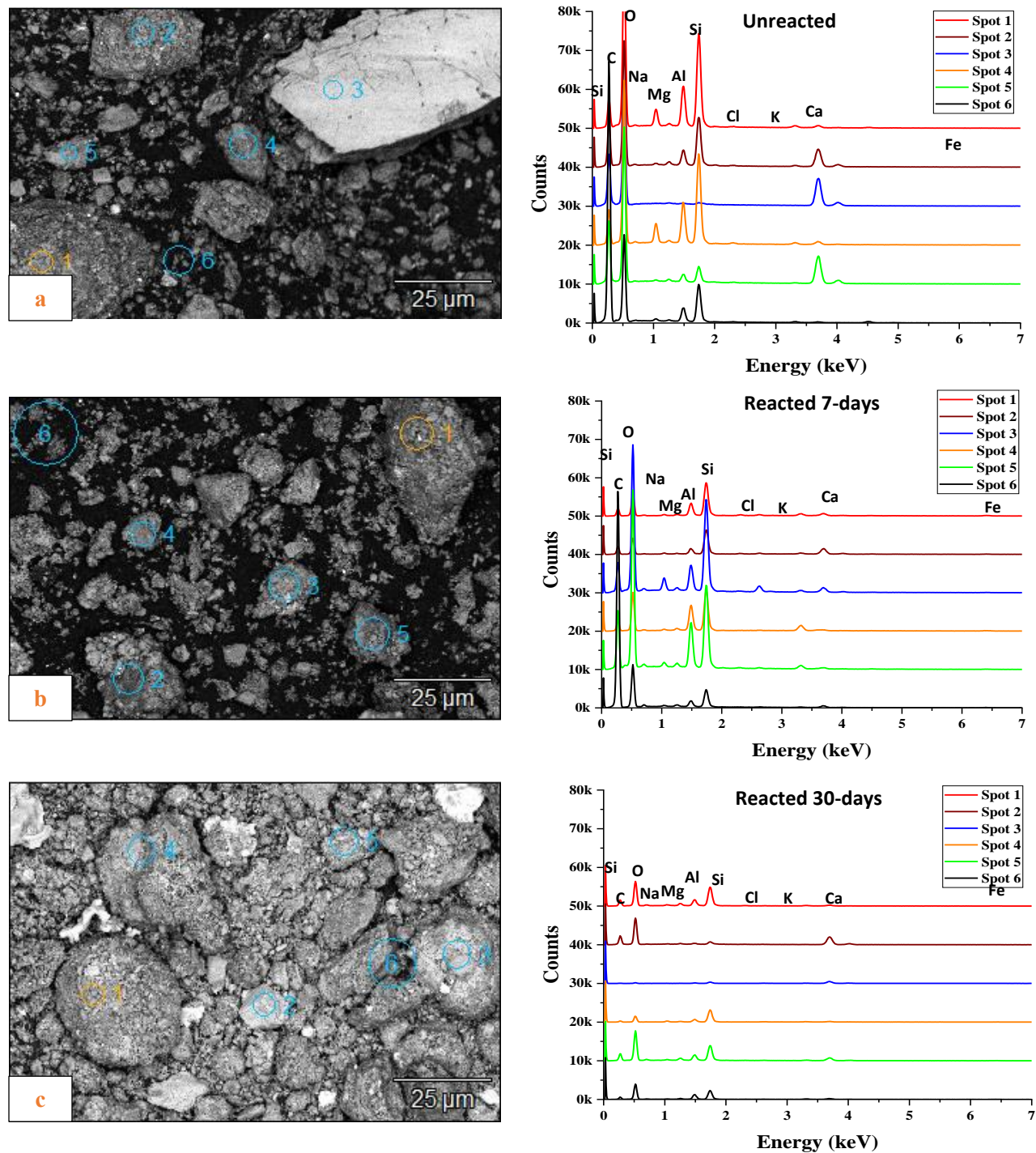


Fig. 4: Comparison of elemental compositions based on spot analyses on powdered samples, for both unreacted and reacted samples. Microanalysis of all samples are conducted under the same conditions. Spectrum 6 in all samples is selected to capture the composition of substrate on which samples are placed. **a.** Unreacted samples show highest peaks for major elemental components, oxygen, silicon, aluminum, and Calcium **b.** Samples reacted for 7-days show peaks for major elemental components reduced compared to unreacted samples. This indicates loss of elements. **c.** Samples reacted for 30-days show lowest peaks for major elements compared to other peaks. The continuous reduction in peaks is due to continuous dissolution of minerals that cause most elements to enter solution.

4.3 Analyses of Reacted Fluid Samples

4.3.1 Analysis of pH

In this experiment, the starting pH of the reactant fluid is approximately neutral, thus reactions do not proceed rapidly compared to other experiments with acid fluids (Bratcher et al. 2021; Li et al. 2020). Trends in pH of samples (Table 3) show marginal decreases after 7-days of reaction and then increases after 30-days reaction. The pH of reacted fluid samples ranged from 6.58 to 6.74 with an outlier of 8.35 after 7-days and between 7.54 to 8.58 after 30-days. The pH of 8.35 after 7-days may be due to rapid breakdown of carbonates in this sample. The decrease in pH can be attributed to the oxidative dissolution of pyrite, which produces sulfuric acid, whilst increases in pH could be attributed to the dissolution of carbonate and clay minerals. Whilst low pH can lead to dissolution of minerals, high pH leads to destabilization of illite which can cause deflocculation and dispersing of illite platelets.

Table 3: pH of fluids over experiment period

Sample	Day 0	Day 7	Day 30
R1	7.13	6.85	7.63
D1	7.13	6.87	7.74
R2	7.13	6.58	7.54
D2	7.13	6.74	8.43
R3	7.13	8.35	8.58

4.3.2 Sodium (Na) Concentration

Concentrations of Na in solution displayed a decreasing trend in the first 7-days but was inconsistent after that (Fig. 5). In some cases, concentration decreased between 7 to 30-days whilst the opposite happens with other samples. The dissolution of feldspar is expected to increase Na concentration; however, the observed decreasing trend of dissolved Na suggests uptake of Na by other mechanisms. The initial decreasing concentrations could be attributed to cation exchange and adsorption to clay mineral surfaces whilst in the later stages, this may be due to precipitation of Na-bearing minerals. Cation exchange is expected to initiate immediately when rock powders and fluids are mixed whilst the dissolution of feldspar would be much slower.

4.3.3 Magnesium (Mg) Concentration

Magnesium concentration assumes a downward trend (Fig. 6) after reacting with rock powders. This trend is consistent with previous published works where synthetic fracturing fluids were used (Awejori et al. 2022). Decreased Mg concentration can be attributed to precipitation of new minerals, exchange in clay interlayer or re-adsorption to clay sites. When compared to the amounts of dissolved Ca, the Mg concentration is relatively low. The impact of dissolved Mg on mineral precipitation may thus be limited. Though XRD analysis captured increases in dolomite content, other Mg-based minerals such as chlorites were not detected, therefore the use of electron microprobe will help to identify trace quantities of other Mg-based minerals that precipitate due to reactions. The main source of Mg in solution is from the breakdown of clay (chlorites) and dolomite. Cation exchange in clay interlayers and desorption from clay surfaces also contributes to dissolved Mg.

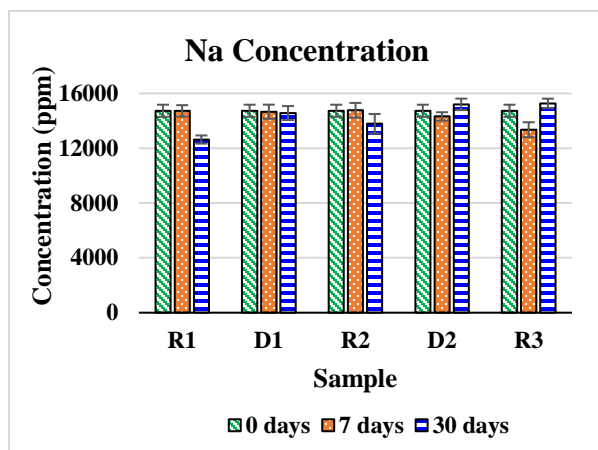


Fig. 5: Na concentration in solution at 0, 7 and 30 days of reaction between rock samples and produced brine. Changes in concentrations are marginal and largely due to re-adsorption of Na in solution as single valence cations are least preferred. Initial concentrations are high.

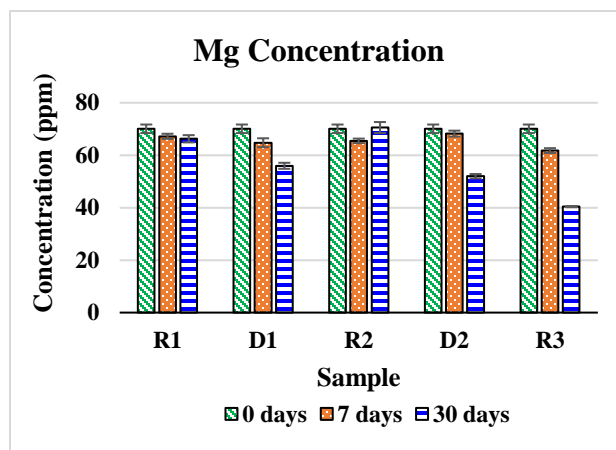


Fig. 6: Mg concentration in solution at 0, 7 and 30 days of reaction between rock samples and produced brine. Declining Mg concentration after few days of reaction may be due to precipitation of Mg bearing minerals albeit in low concentrations, thus undetectable by XRD.

4.3.4 Al Concentration

Al that enters solution is primarily from the dissolution of feldspars and clay minerals as well as exchange in clay sites. Precipitation of illite and other Al-based minerals however cause the decrease in dissolved Al concentrations. From the plots of Al concentration with time (Fig. 7), the Al concentration increased after 7 days reaction and declined by 30-days of reaction to levels observed in pre-reaction fluids. The initial increase is attributable to the dissolution of feldspars and clay minerals during the first few days of reaction whereas during the latter stages, the formation of illite and other Al-based minerals lower the Al concentrations in solution. The increase in illite weight percent as measured by XRD corroborates the trend of Al in solution.

4.3.5 Si Concentration

Si is a major component of the most predominant minerals and entities in sedimentary rocks and is therefore expected to be found in solution following rock-fluid reactions. The dissolved Si is expected to result from the dissolution of quartz and other silica polymorphs, feldspar, and clay minerals. However, the low solubility of quartz under the present experimental conditions suggest that it is not a major source of Si released in solution. The formation and precipitation of clay minerals are the major reactions that lead to consumption of Si in solution. In these rock-fluid reactions, the dissolved Si concentration continues to increase as observed from the graphs in Fig. 8. A plausible reason for high dissolved Si concentrations in the experiments is the dissolution of biogenic silica, which has a much higher solubility than quartz and could easily dissolve during rock-fluid interactions. The presence of biogenic silica in the Caney Shale has been established by earlier research (Milad et al. 2020; Milad and Slatt 2019; Rush 2016).

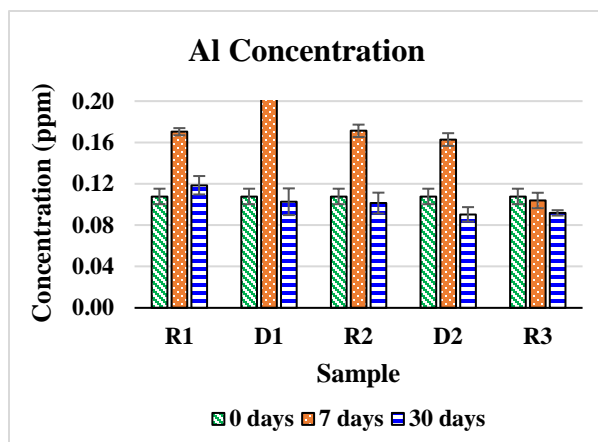


Fig. 7: Al concentration in solution at 0, 7 and 30 days of reaction between rock samples and produced brine. Initial increased concentrations after 7 days due to breakdown of feldspar whilst later decline due to precipitation of Al bearing minerals like illite (clay).

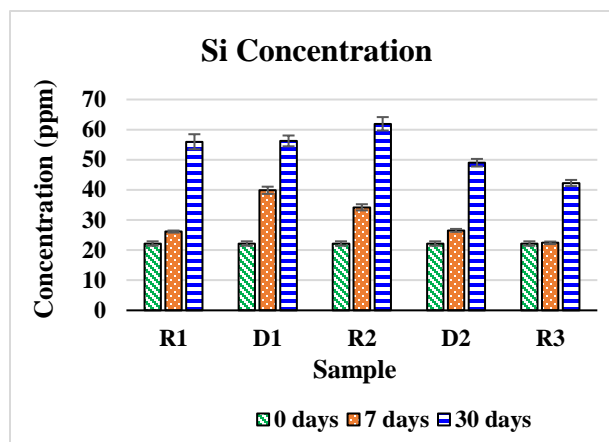


Fig. 8: Si concentration in solution after 0, 7 and 30 days of reaction between rock samples and produced brine. The general trend shows increased Si concentration with time due to breakdown of feldspar, biogenic silica, and amorphous silica.

4.3.6 K Concentration

The K concentration in solution is likely predominantly from the dissolution of feldspars and from clay exchange sites. Although the main feldspar type detected by XRD is plagioclase feldspar, potassium-feldspar is also present, albeit in quantities below XRD detection limits in our case ($< \sim 2\%$). Observing from the graphs of K concentration trends, the initial increase is attributed to the dissolution of K-feldspars and clay minerals. The initial increase of K concentration in the first 7-days of reaction is followed by a decline between 7 to 30-days (Fig. 9) which can be attributed to uptake of K cations in stabilization of clay minerals as well as in the precipitation of new minerals. The predominant clay mineral in the rock is illite, which is stabilized by absorbing K cations into its interlayer. Though not conclusive, the increase in composition of illite after 7-days reaction suggest the precipitation of illite, which would have involved the consumption of K ions in solution.

4.3.7 Ca Concentration

The evolution of Ca concentrations in solution is influenced by the dissolution of calcite, dolomite, and possibly feldspar and some clay minerals. Formation and precipitation of new minerals may also take up Ca already in solution, for example, by the formation of gypsum ($\text{CaSO}_4 \cdot 2\text{H}_2\text{O}$). Another source of Ca fluctuations in solution is exchange on clay surfaces and interlayer ion exchanges. In this study, as illustrated on the graphs (Fig. 10), Ca concentrations decrease after 7-days of reaction, but these trends are reversed for most samples between 7-days to 30-days. The relative stability of Ca in these reactions results from the initial high concentrations of Ca in produced brines and the circumneutral pH of these fluids at the onset of reaction. The trend of dissolved Ca concentrations corroborates the results obtained from XRD measurements in terms of mineralogical changes of carbonate minerals after reacting with fluids for both 7-days and 30-days. The beginning of carbonate minerals dissolution in these experiments is therefore thought to be largely influenced by dissolution of pyrite which causes transient acidity locally to dissolve proximal carbonates.

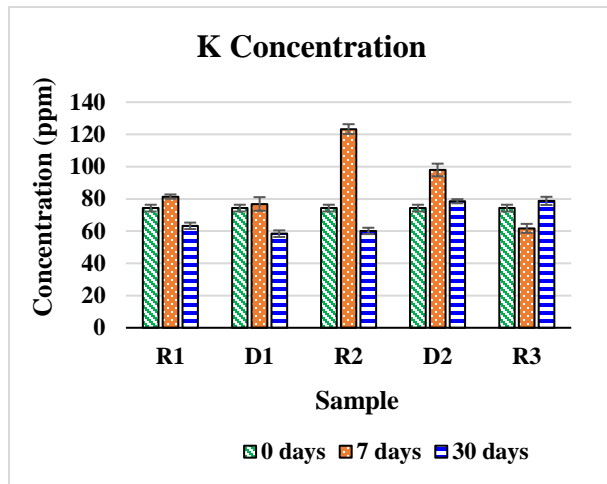


Fig. 9: K concentration in solution at 0, 7 and 30 days of reaction between rock samples and produced brine. Initial increase of K for some samples after 7 days is due to dissolution of feldspars. K is later absorbed to stabilize illite.

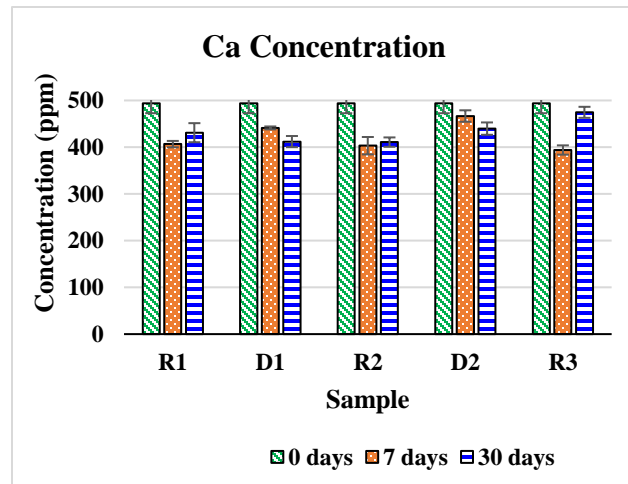


Fig. 10: Ca concentration in solution after 0, 7 and 30 days of reaction between rock samples and produced brine. Initial high Ca concentration declines due to cation exchange whilst increases after 30 days due to localized calcite breakdown.

4.3.8 Fe Concentration

Iron is a ubiquitous element in sedimentary minerals and mostly integrated into most clay minerals. The presence of iron in reacted fluid samples is therefore mostly a given. In this study, iron concentration declined rapidly after 7-days and 30-days of reaction (Fig. 11). The initially high concentrations of Fe in produced brine are from breakdown of iron bearing minerals such as pyrite and possibly Fe-bearing carbonates (siderite, ankerite). After release in solution, Fe(II) is oxidized to Fe(III) and followed by the precipitation of ferric oxyhydroxides. These can form scales that will negatively affect the permeability of the reservoir. The oxidation process is enhanced by the presence of organic compounds from bitumen in rock powder samples (Jew et al. 2017).

4.3.9 Sr Concentration

Strontium is mostly present in the reservoir formation as part of carbonate minerals or adsorbed onto clay surfaces. It is released in solution during reaction primarily by the dissolution of carbonates, clays, and desorption from clay surfaces. The trend of dissolved Sr concentrations (Fig. 12) shows concentrations increasing marginally after 7 days before declining by 30 days. Initial increases in Sr concentrations are likely due to exchange in clay sites since the dissolution of carbonates is expected to be slower. The decline, however, could be the result of formation of Sr-based minerals such as celestite, which readily precipitate in the presence of sulfates, albeit in trace quantities for this reaction since the mineral was not detected in XRD analysis. Celestite is known to cause permeability impairment in reservoirs (Mackay 2003; Shojaee et al. 2023; Tranter et al. 2021).

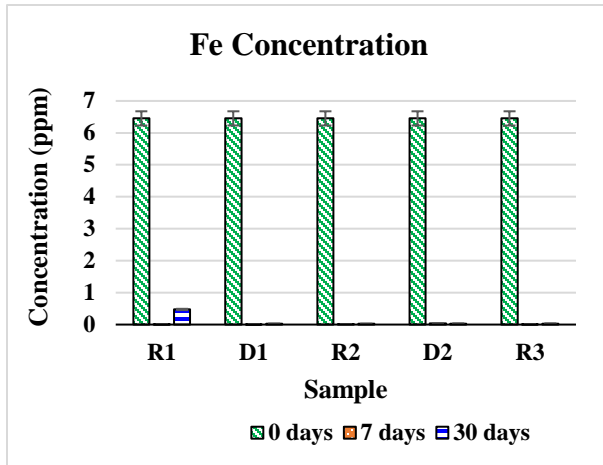


Fig. 11: Fe concentration in solution at 0, 7 and 30 days of reaction between rock samples and produced brine. Fe concentration drops rapidly due to precipitation of Fe minerals.

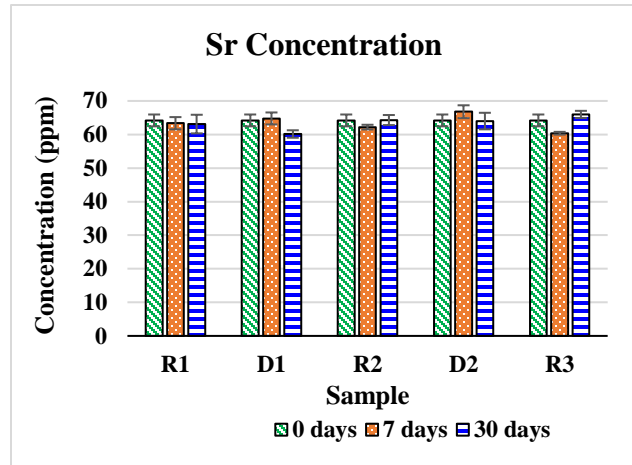


Fig. 12: Sr concentration in solution at 0, 7 and 30 days of reaction between rock samples and produced brine. Sr concentrations are relatively stable with slight shifts throughout the experiments.

4.3.10 Ba Concentration

Barium is generally adsorbed onto clay mineral surfaces and is released into solution due to breakdown of clay or ion exchange (Renock et al. 2016; Zhang et al. 2001). The behavior of barium in solution has been evaluated and documented by many researchers who have all averred that barium reacts with sulfates in solution to form barite, which precipitates and can occlude flow paths in the reservoir. The precipitation of barite has been identified as one of the most common reservoir damage mechanisms (Dieterich et al. 2016; Kumar et al. 2018; Osselin et al. 2019). In this study, the trends of Ba in solution (Fig. 13) largely support its initial release followed by the precipitation of barite, which is corroborated by the EDS elemental analysis though evidence of barite precipitation was not observed in XRD mineralogical analysis. This may be due to the presence of only trace amounts of barite in rock powders.

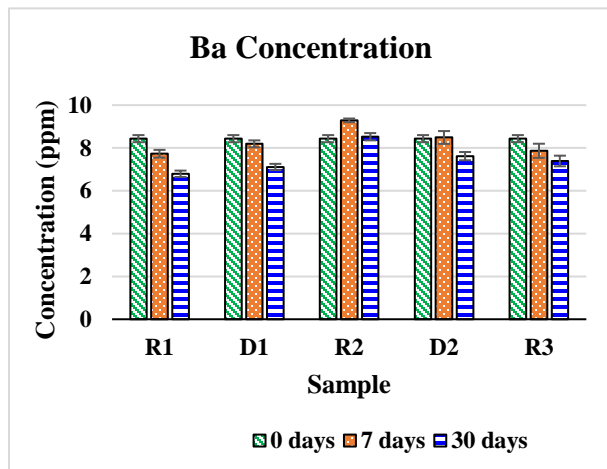


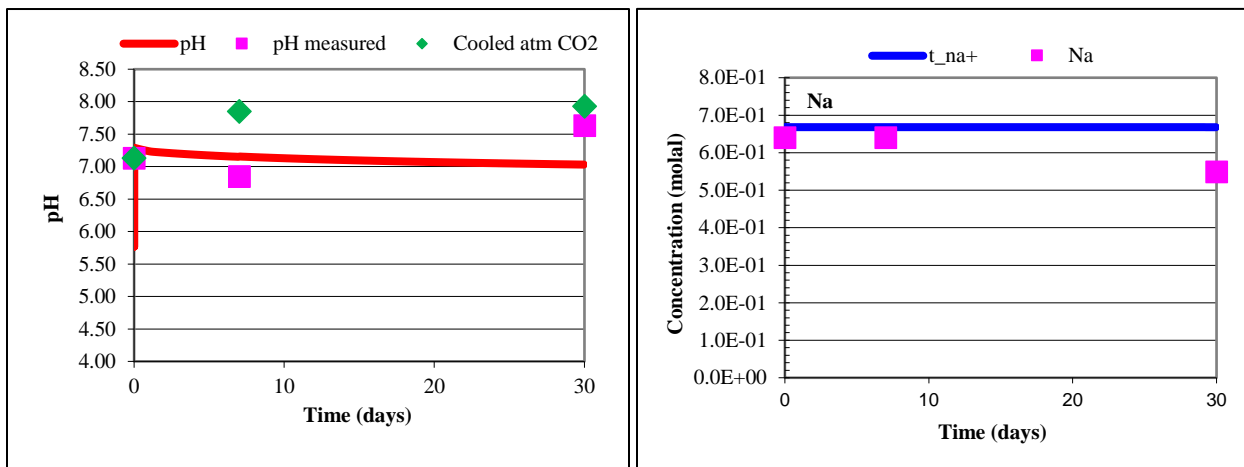
Fig. 13: Ba concentration in solution at 0, 7 and 30 days of reaction between rock samples and produced brine. Declining concentrations caused by precipitation of barite or adsorption by clays.

4.4 Modelling Results

Geochemical modelling of experiments largely supported the results from experiments, though the modelling showed relatively less reaction. Representative modelling results are shown in Fig. 14 for the case of reaction with produced brine and discussed below. Generally, the modelled trends observed for reaction with produced brines showed much less reaction compared to reactions simulated with DI water. This is shown by the almost flat curves observed on the modelled trends in Fig. 14. The less reactivity of produced brines relative to DI water is expected because the produced brines already reacted with rocks in the formation and have compositions that are closer to equilibrium with formation. It is however worth noting that the model results shown here are subject to uncertainties, including the reconstruction of the produced brine composition, mineral reactive surface areas (calibrated using the experiments with DI water), the composition and quantities of trace minerals in the shale (which would be below the detection limit of XRD), redox conditions (estimated by adjusting O_2 partial pressure to best match the experiments), as well as input thermodynamic data.

Modelling the reaction of shale with produced brine showed minimal reactions. The elemental concentrations of Na, K, Mg and Ca are essentially flat, which is an indication of minimal to no reaction between the shale samples and produced brines. The model also showed that most clay minerals were close to equilibrium with the produced brine which confirms the constant concentrations of elements observed in the model. The oxidative dissolution of pyrite in the model is succeeded by the precipitation of Fe (oxy)hydroxides (modeled as ferrihydrite), which seems to be consistent with the observed initially high, then decreasing, dissolved Fe concentrations in the experiments.

The dissolved Al in the model was found to quickly reprecipitate as Al hydroxide (modeled here as gibbsite), while all simulations underpredicted the dissolved Al concentration. This is probably because the precipitation rate of the modeled Al hydroxide is too high, or because the type of secondary Al phase might not be gibbsite. Precipitation of small amounts of illite, montmorillonite and kaolinite were also found to form in the model in cases with > 10 vol% plagioclase in the reacted shale sample. Fig. 14 below shows the comparison of modelled trends of elemental concentrations relative to experimental results.



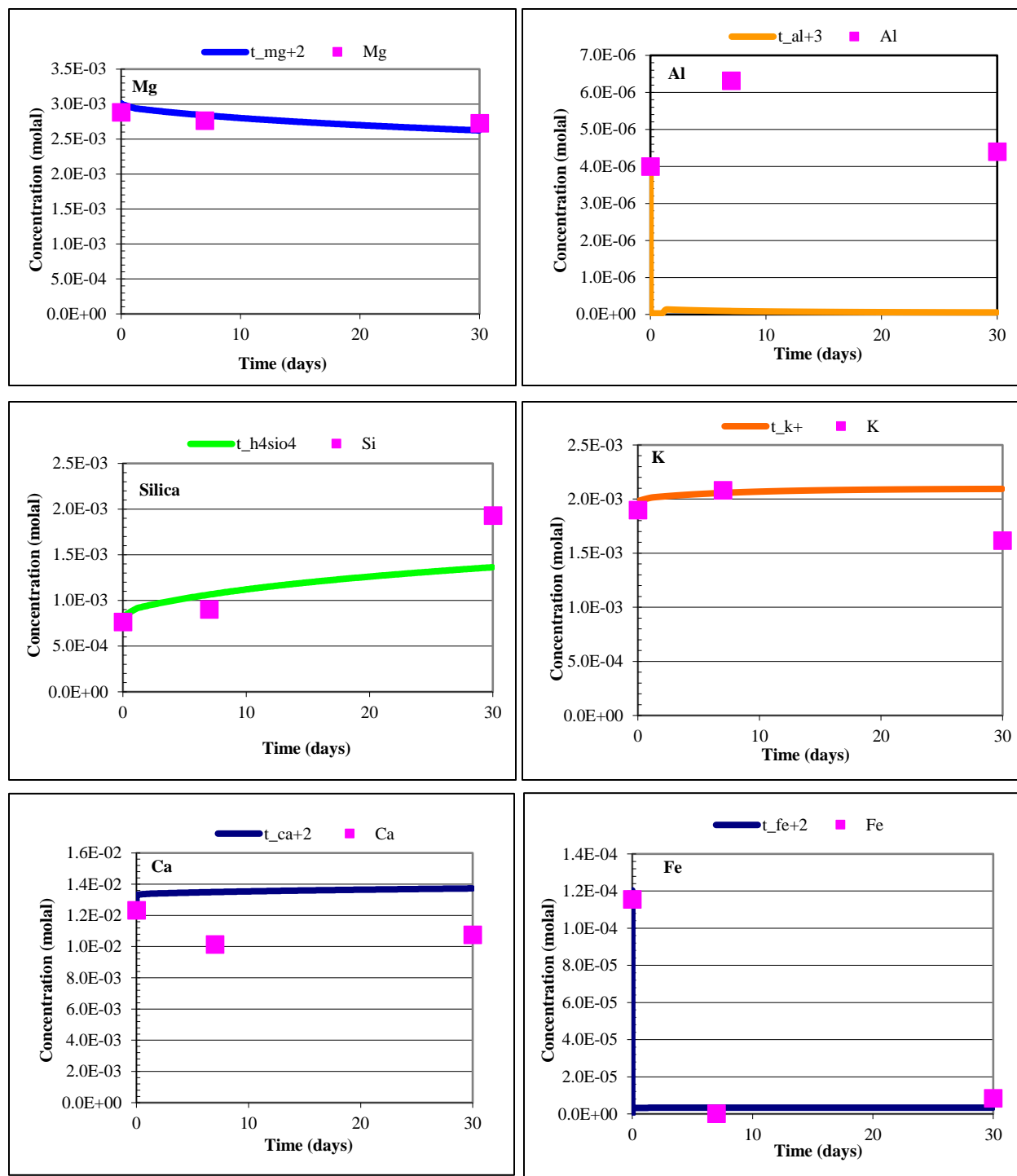


Fig. 14. Example of modeled (lines) and measured (squares) solution compositions (experiment R1). The final modeled pH (at 95°C) was numerically cooled to 25°C (diamond symbols) for comparison with the measurements.

5.0 Discussions

5.1 Illitization

Illitization refers to the precipitation of illite in the subsurface. This process has been identified to occur during deposition and diagenesis with significant impact on petrophysics of the reservoir (Berger et al. 1997; Drief et al. 2002; Ehrenberg and Nadeau 1989; Lázaro 2007; Ohazuruike and Lee 2023). Studies on post-fracturing geochemical reactions in reservoirs have revealed the potential of this phenomenon with considerable adverse effects on reservoir petrophysics (Creodoz et al. 2011; Güven et al. 1982; Huang et al. 1986; Vidal et al. 2017). Illite precipitation can be attributed to the breakdown of feldspar and transformation of smectite. While feldspar dissolution could create higher porosity and permeability (Heald and Larese 1973; Herz-Thyhsen et al. 2019, 2020; Van de Kamp 2008; Worden and Morad 1999), the formation of illite resulting from these reactions poses deleterious impact on the petrophysics of the formations (Stalder 1973).

The potential for illitization during and after hydraulic fracturing were demonstrated by Creodoz et al. (2011), Huang et al. (1986) and Güven et al. (1982) in their experiments where common formation minerals were reacted with simplified fracturing fluids at reservoir conditions. They observed that illitization was intense within acidic to moderate pH regions, due to proton-promoted illitization and thermal effects respectively. Huang et al. (1986) identified the specific conditions that favor illitization. They proffered that formation of illite is favored by high Al concentrations at circum-neutral pH. The geochemical processes leading to this is an initially highly acidized fluid environment which yields high Al concentrations in solution with subsequent titration to obtain a high fluid/rock ratio and circum-neutral conditions in the reservoir. This is similar to the dynamics that exist during hydraulic fracturing, thus the potential for illitization.

Results from batch experiments show illite composition increasing in the first 7-days and decreasing marginally between 7-days to 30-days. Although the produced brine is not initially acidized, the breakdown of pyrite introduces localized transient aciditification which causes breakdown of feldspar to generate sufficient Al in solution to trigger illitization. The reduction in Al concentrations in solution over time decreases the rate of illitization causing marginal decrease or stabilized illite compositions between 7-days to 30-days.

5.2 Biogenic Silica Solubility

Several studies have confirmed the formation and presence of biogenic silica in sedimentary rocks (Buesseler 1998; Crawford et al. 2001; Fishman et al. 2013; Hesse 1988; Hildebrand 2004; Kröger and Sumper 2000; Siever 1992; Wise Jr and Weaver 1975). Biogenic silica constitutes a major component of organic sediments in marine sedimentary rocks after calcium carbonate and is often attributed to unicellular diatoms (Cwienk 1986). The disordered structure of biogenic silica makes it difficult to detect during XRD, and in some cases its structure is amorphous (Richard Drees et al. 1989). Temperature and pressure conditions are critical to the solubility of biogenic silica. Solubility increases between 70% to 100% within the temperature range of 3°C to 23°C and may increase by up to 20% within depth ranges observed in oceans compared to ambient conditions (Kamatani 1982; Lawson et al. 1978; Willey 1974). Other factors affecting the solubility of biogenic silica include the adsorbed cations on the surface of the silica and the aluminum content during formation of the biogenic silica. Solubility reduces with increasing adsorbed cations and reduces when cations are removed mostly by acid action (Lewin 1961). Increased aluminum or

high Al/Si ratio also causes solubility to decrease, thus the biogenic silica formed in beach environments tends to be less soluble than that formed in the open ocean (Van Bennekom et al. 1991).

Basin evolution records of the Caney Formation of the Ardmore Basin show depositional environments of coastal and shallow marine origins (Fritz et al. 2012) that greatly favored the formation and preservation of diatoms, thus biogenic silica content. The trends observed in silica concentration during rock-fluid interactions also show signatures of high content of biogenic silica.

5.3 Scale Formation

During and after hydraulic fracturing, through shut in and production, fracturing fluids come in contact with formation fluids and rocks creating reactions which lead to the dissolution of minerals. The dissolution of these minerals releases ions into solution and under the right conditions and saturation, new minerals are precipitated. Most of the precipitated minerals form scales on fracture walls which eventually narrows flow paths of fluids (Al Rawahi et al. 2017; Hakala et al. 2021b). Based on trends in elemental concentrations in reactant fluids used in this experiment, the potential for scale formation is examined below.

5.3.1 Carbonate Scale

Carbonates are mostly present in formation rocks as calcite and dolomite with minor amounts of other forms of carbonates (e.g., siderite, ankerite), mostly as cements within inter-particle and intra-particle spaces (Leighton and Pendexter 1962; Ling et al. 2014). During and after hydraulic fracturing, carbonate minerals are dissolved. The dissolution is intense in highly acidic environments created by the injection of highly acid fracturing fluids. Upon pH neutralization away from injection zones, carbonate anions combine with cations in solution to precipitate and form scales, which obstruct flow of hydrocarbons. The formation of these carbonate scales depends largely on pH, temperature, and pressure conditions apart from the presence of high concentrations of the constituent ions. Carbonate scale deposition has been reported to increase with increasing pH and temperature and decreasing pressure (Hamid et al. 2016; Jordan et al. 2014; MacAdam and Parsons 2004; Ramstad et al. 2020). Calcite is the most stable form of calcium carbonate scales as compared to aragonite and vaterite. Iron carbonate is another common scale forming carbonate in the formation which occurs due to loss of dissolved CO₂ resulting from changes in temperature and pressure thus increasing the pH of the system. The increased pH reduces the solubility of the carbonate minerals and thus precipitation occurs (Jordan et al. 2014). Strontium ions, which are mostly adsorbed on clay minerals, and a common trace element in calcite, are released into solution through ion exchange and dissolution processes that occur during hydraulic fracturing. Upon pH increase Sr also reacts with carbonate ions to form strontianite. Strontianite is a common scale that occurs in hydrocarbon reservoirs and has been reported by several researchers (Ghalib et al. 2023; Korrani et al. 2014; Spielman-Sun et al. 2021).

5.3.2 Sulfate Scale

During hydraulic fracturing, oxygenated fluids are injected in high quantities into the subsurface formation which is mostly in a reduced state. The presence of oxidants triggers reactions that lead to the breakdown of sulfides and subsequent oxidation to sulfates. These sulfates in the formation react with various cations to form new minerals which can reduce the porosity and permeability of the reservoir. The most common sulfate scale mineral formed in reservoir during and after hydraulic fracturing is barite, which has detrimental impact on the permeability of the formation (Paukert Vankeuren et al. 2017; Xiong et al. 2020). Barite scale formation has been reported in major unconventional producing fields in the USA, including

Marcellus and Eagle Ford (Hakala et al. 2021; Li et al. 2019; Paukert-Vankeuren et al. 2017; Wilson and Van Briesen 2013). Barite precipitation in hydraulically fractured reservoirs is intrinsically associated with drilling fluid additives, the formation rock, and the chemical composition of water used in fracturing (Dieterich et al. 2016; Marcon et al. 2017; Vankeuren et al. 2017). Calcium sulfate is another major sulfate scale reported in hydraulically fractured reservoirs. It causes substantial challenges in relation to formation permeability (Mahmoud 2014). Calcium sulfate can precipitate in three different forms including gypsum, anhydrite, and hemihydrate. These are temperature dependent, and the mineral deposited is dependent on the conditions prevailing in that space. In general, the solubility of calcium sulfate increases with temperature up to 40°C (Moghadasi et al. 2004; Moghadasi et al. 2019) and then reduces with increasing temperature. Gypsum precipitates at lower temperature relative to anhydrite. Under reservoir conditions, the solubility of anhydrite is lower than gypsum, thus anhydrite scale formation is predominant in reservoirs (Isah et al. 2022). Pressure and very minimally pH, also have an impact on the solubility of calcium sulfate. The solubility decreases with increasing pH and lower pressures (Carlberg 1973; Delorey et al. 1996; Moghadasi et al. 2004). Strontium sulfate (Celestite) is another known sulfate scale in hydraulically fractured reservoirs which forms when strontium cations, mostly adsorbed on clay mineral surfaces is released into solution due to ion exchange in clays following hydraulic fracturing. These typically react with sulfates in solution to form celestite (Esteves et al. 2021; Esteves et al. 2022; Spielman-Sun et al. 2021).

5.3.3 Oxide/Hydroxides Scales

The formation of oxyhydroxides following hydraulic fracturing is a common phenomenon in hydraulically fractured reservoirs (Harrison et al. 2017; Jew et al. 2017; Li et al. 2019; Lu et al. 2017). Oxides and hydroxides that have been reported in oilfield reservoirs include iron oxide, aluminum oxide, silicon oxide, strontium oxide, chromium oxide, molybdenum oxide, and iron hydroxide among others (Jew et al. 2017; Jones 1978; Kamal et al. 2018). The most prevalent and problematic oxyhydroxide scale however is iron oxyhydroxide. Iron mineral scale occurs due to the oxidation of Fe (II) from the breakdown of pyrite and reduced iron-bearing minerals. Iron is ubiquitous in unconventional shale formations in a reduced Fe(II) state due to the typically reduced environment in these formations. Fe(II) minerals break down rapidly at the onset of hydraulic fracturing due to the introduction of acid and oxygenated fluids which change the pH and redox conditions in the formation (Ferguson et al. 2021; Kirk Nordstrom 1982; Moses et al. 1987). The breakdown and oxidation of Fe (II) leads to the precipitation of Fe (III) oxides and hydroxides. Fe (III) oxyhydroxide precipitation generally occurs within the rock matrix and extends into the fracture face, thus causing considerable adverse alteration of permeability (Alalli et al. 2018; Li et al. 2020; Li et al. 2019; Li et al. 2019).

6.0 Conclusion

The integration of results from experiments and discussions based on published research led us to the following conclusions:

- Changes in mineralogical compositions of rock samples and elemental concentrations in produced brines indicate reaction between rocks and produced fluids (mixture of fracturing fluid and formation fluid). This provides evidence of potential long-term rock-fluid reaction, given that produced brines and rock are almost in equilibrium.

- The presence of oxygen and remaining oxidants in produced fluids (oxidants originally used as additives in fracturing fluids) has a significant effect on the reaction processes between rocks and fluids.
- The breakdown and oxidation of sulfides (pyrite) causes localized acidization which catalyzes the dissolution of other minerals, especially carbonates.
- Analyses of elemental concentrations in reacted fluids show the presence of iron, barium, strontium, and other cations that could easily react with dissolved carbonate and sulfate to precipitate scale forming minerals that are detrimental to the permeability of the formation. This shows the Caney Shale is susceptible to long-term reservoir damage.
- Changes in elemental concentrations in reacted rock samples, detected by EDS area analyses, suggest that the dissolution of shale minerals contributes to the release elements in solution. In the field, these elements, in the form of ions could subsequently react to precipitate new minerals within micro-fractures, which could lead to a significant drop in reservoir permeability.
- The relative increase in illite content in reacted samples in the experiments indicates a high potential for clay fines migration in the shale formation in the long-term as illite may subsequently physically breakdown in fine particles at higher pH conditions (Ahmad et al. 2018).
- The relative increase in illite content in rock-powders after reacting with produced fluid suggests that in the field, such illitization could shift the properties of the reservoir rock, from a relatively brittle rock into a relatively ductile rock. This transformation within the reservoir will enhance fracture healing in the long-term, and thus reduce permeability.

Declarations

Ethics Approval

- The authors declare that all ethical and professional conduct have been adhered to and complied with in this study.

Conflict of Interest

- We declare that the authors of this manuscript have no conflict of interest as defined by Springer, or other interests that might be perceived to influence the results and/or discussion reported in this paper.

Data Availability

- The authors declare that the data supporting the findings of this study are available within the paper. Details of meta-data of the presented data are available from corresponding author on request.

Author Contribution

- Gabriel Adua Awejori was involved in conceptualization, laboratory experiment, data acquisition, data presentation, data interpretation, writing main manuscript text, compiling the manuscript, and editing of manuscript.
- Dr. Wenming Dong was involved in, data acquisition, data presentation, writing part of methodology, and editing of manuscript.

- Dr. Christine Doughty was involved in supervision, conceptualization, data interpretation, and editing of manuscript.
- Dr. Nic Spycher was involved in conceptualization, modelling, writing part of methodology, data interpretation, and editing manuscript.
- Dr. Mileva was involved in acquisition of funding, supervision, conceptualization, laboratory experiment, data acquisition, data interpretation, and editing of manuscript.

Funding

- This study was funded by the US Department of Energy (DOE), Office of Fossil Energy, Award DE-FE0031776.

Consent to Publish

- All authors presented in this manuscript have provided their consent for this study to be submitted and published upon acceptance.

References

- Ahmad KM, Kristály F, Turzo Z, Docs R (2018) Effects of clay mineral and physico-chemical variables on sandstone rock permeability. *J Oil Gas Petrochem Sci*, 1(1), 18–26
- Al Rawahi YM, Shaik F, Rao LN (2017) Studies on scale deposition in oil industries and their control. *International Journal for Innovative Research in Science & Technology*, 3(12), 152–167
- Alalli A, Li Q, Jew A, Kohli A, Bargar J, Zoback M, Kovscek A (2018) Effects of hydraulic fracturing fluid chemistry on shale matrix permeability. *SPE/AAPG/SEG Unconventional Resources Technology Conference*
- Alfarge D, Wei M, Bai B (2019) Evaluating the performance of hydraulic fractures in unconventional reservoirs using production data: Comprehensive review. *Journal of Natural Gas Science and Engineering*, 61, 133–141
- Alkough A, Wattenbarger RA (2013) New advances in shale reservoir analysis using flowback data. *SPE Eastern Regional Meeting*
- Appelo CAJ, Postma D (2005) *Geochemistry, groundwater and pollution: Leiden, The Netherlands* AA Balkema Publishers
- Arnorsson S, Stefansson A (1999) Assessment of feldspar solubility constants in water in the range of 0 degrees to 350 degrees C at vapor saturation pressures. *American Journal of Science*, 299(3), 173–209
- Aslannezhad M, Kalantariasl A, You Z, Iglauer S, Keshavarz A (2021) Micro-proppant placement in hydraulic and natural fracture stimulation in unconventional reservoirs: A review. *Energy Reports*, 7, 8997–9022
- Awan FUR, Keshavarz A, Akhondzadeh H, Al-Anssari S, Iglauer S (2020) A novel approach for using silica nanoparticles in a proppant pack to fixate coal fines. *The APPEA Journal*, 60(1), 88–96

- Awan FUR, Keshavarz A, Azhar MR, Akhondzadeh H, Ali M, Al-Yaseri A, Abid HR, Iglauer S (2021) Adsorption of nanoparticles on glass bead surface for enhancing proppant performance: A systematic experimental study. *Journal of Molecular Liquids*, 328, 115398
- Awejori GA, Doughty C, Xiong F, Paronish T, Spycher N, Radonjic M (2022) Integrated Experimental and Modelling Study of Geochemical Reactions of Simple Fracturing Fluids with Caney Shale. *Energy & Fuels*, 36(17), 10064–10081
- Awejori GA, Luo G, Grider C, Katende A, Radonjic M, Doughty C, Spycher N, Paronish T, O'Connell L, Rihn A (2021) Fracturing Fluid-Induced Mineralogy Changes and Impact on Elastic Properties for the Caney Shale, Oklahoma. *55th US Rock Mechanics/Geomechanics Symposium*
- Barbot E, Vidic NS, Gregory KB, Vidic RD (2013) Spatial and temporal correlation of water quality parameters of produced waters from Devonian-age shale following hydraulic fracturing. *Environmental Science & Technology*, 47(6), 2562–2569
- Bedrikovetsky P, Keshavarz A, Khanna A, Kenzie KM, Kotousov A (2012) Stimulation of natural cleats for gas production from coal beds by graded proppant injection. *SPE Asia Pacific Oil and Gas Conference and Exhibition*
- Bennour Z, Ishida T, Nagaya Y, Chen Y, Nara Y, Chen Q, Sekine K, Nagano Y (2015) Crack extension in hydraulic fracturing of shale cores using viscous oil, water, and liquid carbon dioxide. *Rock Mechanics and Rock Engineering*, 48, 1463–1473
- Berger G, Lacharpagne JC, Velde B, Beaufort D, Lanson B (1997) Kinetic constraints on illitization reactions and the effects of organic diagenesis in sandstone/shale sequences. *Applied Geochemistry*, 12(1), 23–35
- Blanc P, Lassin A, Piantone P, Azaroual M, Jacquemet N, Fabbri A, Gaucher EC (2012) Thermoddem: A geochemical database focused on low temperature water/rock interactions and waste materials. *Applied Geochemistry*, 27(10), 2107–2116
- Bo L, Mingxiu C, Yuanyuan L, Jinpeng X, Yueming Q, Liqiang M (2023) Mechanism and factors controlling spontaneous imbibition of simulated fracturing fluid into synthetic shales. *Environmental Earth Sciences*, 82(12), 287
- Bol GM, Wong SW, Davidson CJ, Woodland DC (1994) Borehole stability in shales. *SPE Drilling & Completion*, 9(02), 87–94
- Bratcher JC, Kaszuba JP, Herz-Thyhsen RJ, Dewey JC (2021) Ionic Strength and PH Effects on Water-Rock Interaction in an Unconventional Siliceous Reservoir: On the Use of Formation Water in Hydraulic Fracturing. *Energy Fuels*, 35, 18414
- Buesseler KO (1998) The decoupling of production and particulate export in the surface ocean. *Global Biogeochemical Cycles*, 12(2), 297–310 <https://doi.org/10.1029/97GB03366>
- Cai Z, Li L (2016) How long do natural waters “remember” release incidents of Marcellus Shale waters: a first order approximation using reactive transport modelling. *Geochemical Transactions*, 17, 1–15
- Cai Z, Wen H, Komarneni S, Li L (2018) Mineralogy controls on reactive transport of Marcellus Shale waters. *Science of the Total Environment*, 630, 1573–1582

- Carlberg BL (1973) Solubility of calcium sulfate in brine. *SPE International Conference on Oilfield Chemistry*, SPE-4353
- Carpenter KC, Dje LB, Achang M, Radonjic M (2023) Comparative Laboratory Study of the Geochemical Reactivity of the Marcellus Shale: Rock–Fluid Interaction of Drilled Core Samples vs. Outcrop Specimens. *Water*, 15(10), 1940
- Cheng Q, Kang Y, You L, Yang P, Zhang X, Cheng Q (2017) Change in composition and pore structure of Longmaxi black shale during oxidative dissolution. *International Journal of Coal Geology*, 172, 95–111
- Cheng Q, You L, Kang Y, Zhang N, Zhou Y (2021a) An experimental investigation into the oxidative dissolution of typical organic-rich shale from China. *Marine and Petroleum Geology*, 130, 105117
- Cheng Q, You L, Kang Y, Zhou Y, Zhang N (2021b) Oxidative dissolution kinetics of organic-rich shale by hydrogen peroxide (H₂O₂) and its positive effects on improving fracture conductivity. *Journal of Natural Gas Science and Engineering*, 89, 103875
- Crawford S, Higgins M, Mulvaney P, Wetherbee R (2001) Nanostructure of the Diatom Frustule as Revealed by Atomic Force and Scanning Electron Microscopy. *Journal of Phycology*, 37, 543–554 <https://doi.org/10.1046/j.1529-8817.2001.037004543x>
- Creoz A, Bildstein O, Jullien M, Raynal J, Trotignon L, Pokrovsky O (2011) Mixed-layer illite–smectite reactivity in acidified solutions: Implications for clayey caprock stability in CO₂ geological storage. *Applied Clay Science*, 53(3), 402–408
- Cwienk DS (1986) *Recent and glacial age organic carbon and biogenic silica accumulation in marine sediments*
- Czerewko MA, Cripps JC (2023) Implications of sulfur mineralogy and consequences of pyrite oxidation for ground engineering. *Journal of the Geological Society*, 180(4), jgs2022-101
- de Farias Esteves B, Li Q, Spielman-Sun E, Jew A, Bargar J, Druhan J (2021) A reactive transport model for celestite precipitation in shale reservoirs subject to hydraulic fracturing. *AGU Fall Meeting Abstracts, 2021*, H55B-0757
- Delorey JR, Allen S, McMaster L (1996) Precipitation of calcium sulphate during carbonate acidizing: minimizing the risk *Annual Technical Meeting*
- Dieterich M, Kutchko B, Goodman A (2016) Characterization of Marcellus Shale and Huntersville Chert before and after exposure to hydraulic fracturing fluid via feature relocation using field-emission scanning electron microscopy. *Fuel*, 182, 227–235
- Drief A, Martinez-Ruiz F, Nieto F, Sanchez NV (2002) Transmission Electron Microscopy evidence for experimental illitization of smectite in K-enriched seawater solution at 50°C and basic pH. *Clays and Clay Minerals*, 50(6), 746–756
- Du H, Carpenter K, Hui D, Radonjic M (2017) Microstructure and micromechanics of shale rocks: Case study of marcellus shale. *Facta Universitatis, Series: Mechanical Engineering*, 15(2), 331
- Du H, Radonjic M, Chen Y (2020) Microstructure and micro-geomechanics evaluation of Pottsville and Marcellus shales. *Journal of Petroleum Science and Engineering*, 195, 107876

- Ehrenberg SN, Nadeau PH (1989) Formation of diagenetic illite in sandstones of the Garn Formation, Haltenbanken area, mid-Norwegian continental shelf. *Clay Minerals*, 24(2), 233–253
- Esteves BF, Spielman-Sun E, Li Q, Jew AD, Bargar JR, Druhan JL (2022) Geochemical Modelling of Celestite (SrSO₄) Precipitation and Reactive Transport in Shales. *Environmental Science & Technology*, 56(7), 4336–4344
- Fakcharoenphol P, Kurtoglu B, Kazemi H, Charoenwongsa S, Wu YS (2014) The effect of osmotic pressure on improved oil recovery from fractured shale formations. *SPE Unconventional Resources Conference/Gas Technology Symposium*, D021S003R004
- Fan L, Thompson JW, Robinson, JR (2010) Understanding gas production mechanism and effectiveness of well stimulation in the Haynesville Shale through reservoir simulation. *Canadian Unconventional Resources and International Petroleum Conference*
- Farhadzadeh M, Nick HM (2023) The critical role of fracture flow on two-phase matrix–fracture transfer mechanisms. *Advances in Water Resources*, 179, 104509
- Ferguson B, Agrawal V, Sharma S, Hakala JA, Xiong W (2021) Effects of Carbonate Minerals on Shale-Hydraulic Fracturing Fluid Interactions in the Marcellus Shale. *Frontiers in Earth Science*, 9, 695978
- Fishman NS, Ellis GS, Boehlke AR, Paxton ST, Egenhoff SO (2013) *Gas storage in the Upper Devonian–Lower Mississippian Woodford Shale, Arbuckle Mountains, Oklahoma: How much of a role do chert beds play?*
- Fritz RD, Medlock P, Kuykendall MJ, Wilson JL (2012) *The geology of the Arbuckle Group in the midcontinent: Sequence stratigraphy, reservoir development, and the potential for hydrocarbon exploration*
- Fritz SJ (1986) Ideality of clay membranes in osmotic processes: a review. *Clays and Clay Minerals*, 34, 214–223
- Ghalib HB, Al-Hawash AB, Muttashar WR, Bozdog A, Al-Saady AA (2023) Determining the effect of mineral scaling formation under different injection water sources on the performance of Mishrif carbonate reservoir in Halfaya oilfield, Southern Iraq. *Journal of Petroleum Exploration and Production Technology*, 13(5), 1265–1282
- Ghanbari E, Abbasi MA, Dehghanpour H, Bearinger D (2013) Flowback volumetric and chemical analysis for evaluating load recovery and its impact on early-time production. *SPE Canada Unconventional Resources Conference*, SPE-167165
- Grieser B, Wheaton B, Magness B, Blauch M, Loghry R (2007) Surface reactive fluid's effect on shale. *SPE Oklahoma City Oil and Gas Symposium/Production and Operations Symposium*, SPE-106815
- Gundogar AS, Ross CM, Jew AD, Bargar JR, Kovscek AR (2021) Multiphysics investigation of geochemical alterations in Marcellus shale using reactive core-floods. *Energy & Fuels*, 35(13), 10733–10745
- Güven N, Lafon GM, Lee LJ (1982) *Experimental hydrothermal alteration of albite to clays: preliminary results*

- Hakala JA, Vankeuren ANP, Scheuermann PP, Lopano C, Guthrie GD (2021) Predicting the potential for mineral scale precipitation in unconventional reservoirs due to fluid-rock and fluid mixing geochemical reactions. *Fuel*, 284, 118883
- Hamid S, De Jesús O, Jacinto C, Izetti R, Pinto H, Droguett E, Edwards C, Cassidy J, Zhang H, Dagenais P (2016) A practical method of predicting calcium carbonate scale formation in well completions. *SPE Production & Operations*, 31(01), 1–11
- Harrison AL, Jew AD, Dustin MK, Thomas DL, Joe-Wong CM, Bargar JR, Johnson N, Brown GE, Maher K (2017) Element Release and Reaction-Induced Porosity Alteration during Shale-Hydraulic Fracturing Fluid Interactions. *Appl Geochem*, 82, 47
- Heald MT, Larese RE (1973) The significance of the solution of feldspar in porosity development. *Journal of Sedimentary Research*, 43(2), 458–460
- Herz-Thyhsen RJ, Kaszuba JP, Dewey JC (2019) Dissolution of minerals and precipitation of an aluminosilicate phase during experimentally simulated hydraulic fracturing of a mudstone and a tight sandstone in the Powder River Basin, WY. *Energy & Fuels*, 33(5), 3947–3956
- Herz-Thyhsen RJ, Kaszuba JP, Dewey, JC (2020) Mineral dissolution and precipitation induced by hydraulic fracturing of a mudstone and a tight sandstone in the Powder River Basin, Wyoming, USA. *Applied Geochemistry*, 119, 104636
- Hesse R (1988) Diagenesis# 13 Origin of chert: Diagenesis of biogenic siliceous sediments. *Geoscience Canada*, 15(3), 171–192
- Hildebrand M (2004) 10 Silicic Acid Transport and its Control During Cell Wall Silicification in Diatoms. *From Biology to Biotechnology and Medical Application*, 159
- Holland TJB, Powell R (1998) An internally consistent thermodynamic data set for phases of petrological interest. *Journal of Metamorphic Geology*, 16(3), 309–343
- Huang WL, Bishop AM, Brown RW (1986) The effect of fluid/rock ratio on feldspar dissolution and illite formation under reservoir conditions. *Clay Minerals*, 21(4), 585–601
- Isah A, Arif M, Hassan A, Mahmoud M, Iglauer S (2022) A systematic review of Anhydrite-Bearing Reservoirs: EOR Perspective, CO₂-Geo-storage and future research. *Fuel*, 320, 123942
- Jew AD, Druhan JL, Ihme M, Kovscek AR, Battiato I, Kaszuba JP, Bargar JR, Brown Jr GE (2022) Chemical and Reactive Transport Processes Associated with Hydraulic Fracturing of Unconventional Oil/Gas Shales. *Chemical Reviews*, 122(9), 9198–9263
- Jew AD, Dustin MK, Harrison AL, Joe-Wong CM, Thomas DL, Maher K, Brown Jr GE, Bargar JR (2017) Impact of organics and carbonates on the oxidation and precipitation of iron during hydraulic fracturing of shale. *Energy & Fuels*, 31(4), 3643–3658
- Jones TS (1978) *Iron Oxide Pigments* (Vol 8771) Department of the Interior, Bureau of Mines
- Jordan MM, Williams H, Linares-Samaniego S, Frigo DM (2014) New insights on the impact of high temperature conditions (176 C) on carbonate and sulphate scale dissolver performance. *SPE International Oilfield Scale Conference and Exhibition*

- Kamal MS, Hussein I, Mahmoud M, Sultan AS, Saad MAS (2018) Oilfield scale formation and chemical removal: A review. *Journal of Petroleum Science and Engineering*, 171, 127–139
- Kamatani A (1982) Dissolution rates of silica from diatoms decomposing at various temperatures. *Marine Biology*, 68(1), 91–96
- Kasiri N, Bashiri A (2011) Wettability and its effects on oil recovery in fractured and conventional reservoirs. *Petroleum Science and Technology*, 29(13), 1324–1333
- Katende A, Allen C, Rutqvist J, Nakagawa S, Radonjic M (2023) Experimental and numerical investigation of proppant embedment and conductivity reduction within a fracture in the Caney Shale, Southern Oklahoma, USA. *Fuel*, 341, 127571
- Katende A, O’Connell L, Rich A, Rutqvist J, Radonjic M (2021) A comprehensive review of proppant embedment in shale reservoirs: Experimentation, modelling and future prospects. *Journal of Natural Gas Science and Engineering*, 95, 104143
- Kazemi-Nia-Korrani A, Sepehrnoori K, Delshad M (2014) A comprehensive geochemical-based approach to quantify the scale problems. *SPE International Conference and Exhibition on Formation Damage Control*, D021S014R002
- Keshavarz A, Badalyan A, Carageorgos T, Bedrikovetsky P, Johnson R (2014) Enhancement of CBM well fracturing through stimulation of cleat permeability by ultra-fine particle injection. *The APPEA Journal*, 54(1), 155–166
- Kirk Nordstrom D (1982) Aqueous pyrite oxidation and the consequent formation of secondary iron minerals. *Acid Sulfate Weathering*, 10, 37–56
- Kröger N, Sumper M (2000) The biochemistry of silica formation in diatoms. *Bio-mineralization*, 151–170
- Kumar S, Naiya TK, Kumar T (2018) Developments in oilfield scale handling towards green technology- A review. *Journal of Petroleum Science and Engineering*, 169, 428–444
- Lawson DS, Hurd DC, Pankratz HS (1978) Silica dissolution rates of decomposing phytoplankton assemblages at various temperatures. *American Journal of Science*, 278(10), 1373–1393
- Lázaro VV (2007) Illitization processes: Series of dioctahedral clays and mechanisms of formation. *Diagenesis and Low-Temperature Metamorphism Theory, Methods and Regional Aspects; Nieto, F, Jiménez-Millán, J, Eds*, 31–39
- Leighton MW, Pendexter C (1962) *Carbonate rock types*
- Lewin JC (1961) The dissolution of silica from diatom walls. *Geochimica et Cosmochimica Acta*, 21(3–4), 182–198
- Li K, Chow K, Horne RN (2002) Effect of initial water saturation on spontaneous water imbibition. *SPE Western Regional/AAPG Pacific Section Joint Meeting*
- Li Q, Jew AD, Brown Jr GE, Bargar JR, Maher K (2020) Reactive transport modelling of shale–fluid interactions after imbibition of fracturing fluids. *Energy & Fuels*, 34(5), 5511–5523
- Li Q, Jew AD, Cercione D, Bargar JR, Brown Jr GE, Maher K (2019) Geochemical modelling of iron (hydr) oxide scale formation during hydraulic fracturing operations. *Unconventional Resources Technology Conference, Denver, Colorado, 22-24 July 2019*, 3863–3876

- Li Q, Jew AD, Kohli A, Maher K, Brown Jr GE, Bargar JR (2019) Thicknesses of chemically altered zones in shale matrices resulting from interactions with hydraulic fracturing fluid. *Energy & Fuels*, 33(8), 6878–6889
- Ling H, Lun Z, Jianxin L, Ji MA, Ruilin LUI, Shuqin W, Wenqi Z (2014) Complex relationship between porosity and permeability of carbonate reservoirs and its controlling factors: A case study of platform facies in Pre-Caspian Basin. *Petroleum Exploration and Development*, 41(2), 225–234
- Lu J, Mickler PJ, Nicot JP, Choi W, Esch WL, Darvari R (2017) Geochemical interactions of shale and brine in autoclave experiments—Understanding mineral reactions during hydraulic fracturing of Marcellus and Eagle Ford Shales. *Aapg Bulletin*, 101(10), 1567–1597
- Lu YH, Chen M, Jin Y, An S, Xie SX, Pan DX, Yuan JB (2012) The development and application of an environmentally friendly encapsulator eba-20. *Petroleum Science and Technology*, 30(21), 2227–2235
- MacAdam J, Parsons SA (2004) Calcium carbonate scale formation and control. *Reviews in Environmental Science & Bio/Technology*, 3, 159–169
- Mackay EJ (2003) Modelling in-situ scale deposition: The impact of reservoir and well geometries and kinetic reaction rates. *SPE Production and Facilities*, 18(01), 45–56
- Mahmoud MA (2014) Evaluating the damage caused by calcium sulfate scale precipitation during low-and high-salinity-water injection. *Journal of Canadian Petroleum Technology*, 53(03), 141–150
- Makhanov K, Habibi A, Dehghanpour H, Kuru E (2014) Liquid uptake of gas shales: A workflow to estimate water loss during shut-in periods after fracturing operations. *Journal of Unconventional Oil and Gas Resources*, 7, 22–32
- Marcon V, Joseph C, Carter KE, Hedges SW, Lopano, CL, Guthrie GD, Hakala, JA (2017) Experimental insights into geochemical changes in hydraulically fractured Marcellus Shale. *Applied Geochemistry*, 76, 36–50
- Mavromatis V, Harrison AL, Eisenhauer A, Dietzel M (2017) Strontium isotope fractionation during strontianite (SrCO₃) dissolution, precipitation and at equilibrium. *Geochimica et Cosmochimica Acta*, 218, 201–214
- Milad B, Slatt R (2019) Outcrop to Subsurface Reservoir Characterization of the Mississippian Sycamore/Meramec Play in the SCOOP Area, Arbuckle Mountains, Oklahoma, USA. *Unconventional Resources Technology Conference, Denver, Colorado, 22-24 July 2019*, 5381–5397
- Milad B, Slatt R, Fuge Z (2020) Lithology, stratigraphy, chemostratigraphy, and depositional environment of the Mississippian Sycamore rock in the SCOOP and STACK area, Oklahoma, USA: Field, lab, and machine learning studies on outcrops and subsurface wells. *Marine and Petroleum Geology*, 115, 104278
- Moghadasi J, Jamialahmadi M, Müller-Steinhagen H, Sharif A (2004) Formation damage due to scale formation in porous media resulting from water injection. *SPE International Conference and Exhibition on Formation Damage Control*, SPE-86524

- Moghadasi R, Rostami A, Tatar A, Hemmati-Sarapardeh A (2019) An experimental study of Nanosilica application in reducing calcium sulfate scale at high temperatures during high and low salinity water injection. *Journal of Petroleum Science and Engineering*, 179, 7–18
- Moses CO, Nordstrom DK, Herman JS, Mills AL (1987) Aqueous pyrite oxidation by dissolved oxygen and by ferric iron. *Geochimica et Cosmochimica Acta*, 51(6), 1561–1571
- Mukhina E, Cheremisin A, Khakimova L, Garipova A, Dvoretzkaya E, Zvada M, Kalacheva D, Prochukhan K, Kasyanenko A, Cheremisin A (2021) Enhanced oil recovery method selection for shale oil based on numerical simulations. *ACS Omega*, 6(37), 23731–23741
- Ohazuruike L, Lee KJ (2023) A comprehensive review on clay swelling and illitization of smectite in natural subsurface formations and engineered barrier systems. *Nuclear Engineering and Technology*
- Osselin F, Saad S, Nightingale M, Hearn G, Desaulty AM, Gaucher EC, Clarkson CR, Kloppmann W, Mayer B (2019) Geochemical and sulfate isotopic evolution of flowback and produced waters reveals water-rock interactions following hydraulic fracturing of a tight hydrocarbon reservoir. *Science of the Total Environment*, 687, 1389–1400
- Palandri JL, Kharaka YK (2004) *A compilation of rate parameters of water-mineral interaction kinetics for application to geochemical modelling*
- Paronish TJ, Schmitt R, Moore JE, Crandall D, Rihn A, Renk J, Doughty C, Bungler A, Wang Y, Katende A (2021) *Computed Tomography Scanning and Geophysical Measurements of the Caney Shale Formation from the Tomaney# 1-35-34-27 Well*. National Energy Technology Laboratory (NETL), Pittsburgh, PA, Morgantown, WV
- Paukert Vankeuren AN, Hakala JA, Jarvis K, Moore JE (2017) Mineral reactions in shale gas reservoirs: barite scale formation from reusing produced water as hydraulic fracturing fluid. *Environmental Science & Technology*, 51(16), 9391–9402
- Pruess K, Oldenburg CM, Moridis GJ (1999) *TOUGH2 user's guide version 2* Lawrence Berkeley National Lab(LBNL), Berkeley, CA (United States)
- Radonjic M, Luo G, Wang Y, Achang M, Cains J, Katende A, Puckette J, Grammer M, King GE (2020). Integrated microstructural characterization of Caney shale, OK. *Unconventional Resources Technology Conference*, 20–22 July 2020, 2157–2174.
- Ramstad K, Sandengen K, Mitchell AF, Moldrheim E (2020) Correlating Calcium Carbonate Scale Risk with Field Experience Data. *SPE International Oilfield Scale Conference and Exhibition*, D011S001R001
- Renock D, Landis JD, Sharma M (2016) Reductive weathering of black shale and release of barium during hydraulic fracturing. *Applied Geochemistry*, 65, 73–86
- Richard Drees L, Wilding LP, Smeck NE, Senkayi AL (1989) Silica in soils: quartz and disordered silica polymorphs. *Minerals in Soil Environments*, 1, 913–974
- Rush W (2016) *Reservoir Characterization and Chemostratigraphy of the Goddard Shale in the South-Central Oklahoma Oil Province*

- Shojaee A, Kord S, Miri R, Mohammadzadeh O (2023) Reactive transport modelling of scale precipitation and deposition during incompatible water injection in carbonate reservoirs. *Journal of Petroleum Exploration and Production Technology*, 1–20
- Siddiqui MAQ, Chen X, Iglauer S, Roshan H (2019) A multiscale study on shale wettability: Spontaneous imbibition versus contact angle. *Water Resources Research*, 55(6), 5012–5032
- Siever R (1992) The silica cycle in the Precambrian. *Geochimica et Cosmochimica Acta* (Vol 56)
- Smith MM, Carroll SA (2016) Chlorite dissolution kinetics at pH 3–10 and temperature to 275 C. *Chemical Geology*, 421, 55–64
- Sonnenthal E, Spycher N, Xu T, Zheng L (2021) *TOUGHREACT V4 12-OMP and TReactMech V1 0 Geochemical and Reactive-Transport User Guide*
- Spielman-Sun E, Jew AD, Druhan JL, Bargar JR (2021) Controlling strontium scaling in the Permian Basin through manipulation of base fluid chemistry and additives. *Unconventional Resources Technology Conference, 26–28 July 2021*, 1292–1301
- Stalder PJ (1973) Influence of crystallographic habit and aggregate structure of authigenic clay minerals on sandstone permeability. *Geologie en Mijnbouw*, 52(4), 217–220
- Stumm W, Morgan JJ (2012) *Aquatic chemistry: chemical equilibria and rates in natural waters* John Wiley & Sons
- Tasker TL, Piotrowski PK, Dorman FL, Burgos WD (2016) Metal associations in Marcellus shale and fate of synthetic hydraulic fracturing fluids reacted at high pressure and temperature. *Environmental Engineering Science*, 33(10), 753–765
- Tranter M, De Lucia M, Kühn M (2021) Barite scaling potential modelled for fractured-porous geothermal reservoirs. *Minerals*, 11(11), 1198
- Tuwiner SB, Miller LP, Brown WE (1962) *Diffusion and membrane technology*, Reinhold Publishing Co
- Van Bennekom AJ, Buma AGJ, Nolting RF (1991) Dissolved aluminium in the Weddell-Scotia Confluence and effect of Al on the dissolution kinetics of biogenic silica. *Marine Chemistry*, 35(1–4), 423–434
- Van de Kamp PC (2008) Smectite-illite-muscovite transformations, quartz dissolution, and silica release in shales. *Clays and Clay Minerals*, 56(1), 66–81
- Vidal J, Patrier P, Genter A, Beaufort D (2017) Occurrences of clay minerals in permeable fracture zones in the granitic basement of geothermal wells at Rittershoffen, France. *42nd Workshop on Geothermal Engineering Stanford University, Stanford, California*
- Wang D, Butler R, Liu H, Ahmed S (2011) Flow-rate behavior and imbibition in shale. *SPE Reservoir Evaluation & Engineering*, 14(04), 505–512
- Wang M, Leung JY (2015) Numerical investigation of fluid-loss mechanisms during hydraulic fracturing flow-back operations in tight reservoirs. *Journal of Petroleum Science and Engineering*, 133, 85–102

- Wang Y, Luo G, Achang M, Cains J, Wethington C, Katende A, Grammer GM, Puckette J, Pashin J, Castagna M (2021) Multiscale characterization of the Caney Shale—an emerging play in Oklahoma. *Midcontinent Geoscience*, 2, 33–53
- Wang Z, Krupnick A (2013) *What Led to the Boom? Resources for the Future US Shale Gas Development What Led to the Boom?*
- Weaver J, Rickman R (2010) Productivity impact from geochemical degradation of hydraulic fractures. *SPE Deep Gas Conference and Exhibition*
- Wilke FDH, Vieth-Hillebrand A, Naumann R, Erzinger J, Horsfield B (2015) Induced mobility of inorganic and organic solutes from black shales using water extraction: Implications for shale gas exploitation. *Applied Geochemistry*, 63, 158–168
- Willey JD (1974) The effect of pressure on the solubility of amorphous silica in seawater at 0 C. *Marine Chemistry*, 2(4), 239–250
- Wilson JM, Van Briesen JM (2013) Source water changes and energy extraction activities in the Monongahela River, 2009–2012 *Environmental Science & Technology*, 47(21), 12575–12582
- Wise Jr SW, Weaver FM (1975) Chertification of oceanic sediments *Pelagic Sediments: On Land and under the Sea*, 301–326
- Worden RH, Morad S (1999) Clay minerals in sandstones: controls on formation, distribution and evolution *Clay Mineral Cements in Sandstones*, 1–41
- Xiong W, Lopano C, Hakala JA, Carney BJ (2020) Investigation of barite scaling during reaction between pre-treated hydraulic fracturing fluid from the field and Marcellus Shale *SPE/AAPG/SEG Unconventional Resources Technology Conference*
- Xu T, Spycher N, Sonnenthal E, Zhang G, Zheng L, Pruess K (2011) TOUGHREACT Version 20: A simulator for subsurface reactive transport under non-isothermal multiphase flow conditions. *Computers & Geosciences*, 37(6), 763–774
- Yang L, Steefel CI (2008) Kaolinite dissolution and precipitation kinetics at 22 C and pH 4. *Geochimica et Cosmochimica Acta*, 72(1), 99–116
- You L, Cheng Q, Kang Y, Chen Q, Dou L, Zhou Y (2018) Imbibition of oxidative fluid into organic-rich shale: implication for oxidizing stimulation. *Energy & Fuels*, 32(10), 10457–10468
- Zeng L, Reid N, Lu Y, Hossain MM, Saeedi A, Xie Q (2020) Effect of the fluid–shale interaction on salinity: implications for high-salinity flowback water during hydraulic fracturing in shales. *Energy & Fuels*, 34(3), 3031–3040
- Zeng YJ, Zhang X, Zhang BP (2015) Stress redistribution in multi-stage hydraulic fracturing of horizontal wells in shales. *Petroleum Science*, 12, 628–635
- Zhang D, Han M, Zhou Q, Ye T, Zhou Y, Chang J, Lin X (2023). The Micro-Occurrence Mechanisms of Tight Oil: Fluid–Rock Interactions at Microscale Pores, Nanoscale Pores, and Mineral Surfaces. *Energies*, 16(9), 3917

- Zhang PC, Brady PV, Arthur SE, Zhou WQ, Sawyer D, Hesterberg DA (2001) Adsorption of barium (II) on montmorillonite: an EXAFS study. *Colloids and Surfaces A: Physicochemical and Engineering Aspects*, 190(3), 239–249
- Zhong C, Leung JY (2020) Numerical investigation of water retention in secondary fractures and apparent permeability modelling in shale gas production. *Journal of Petroleum Science and Engineering*, 192, 107294
- Zhou Z, Abass H, Li X, Bearinger D, Frank W (2016) Mechanisms of imbibition during hydraulic fracturing in shale formations. *Journal of Petroleum Science and Engineering*, 141, 125–132
- Zou C, Zhang G, Zhi Y, Shizhen T, Lianhua H, Rukai Z, Xuanjun Y, Qiquan R, Denghua L, Zhiping W (2013) Concepts, characteristics, potential and technology of unconventional hydrocarbons: On unconventional petroleum geology. *Petroleum Exploration and Development*, 40(4), 413–428

APPENDICES

Appendix A

Table A.1: Mineralogical composition (in weight percent) of unreacted rock powder samples.

Initial Mineralogy (0-days)							
Sample	Quartz (%)	Calcite (%)	Dolomite (%)	Pyrite (%)	Albite (%)	Illite (%)	Ankerite (%)
R1	57.5	8.5	1.9	1.5	5.7	23	1.9
D1	54.2	6.1		1.7	8.8	29.2	
R2	15.9	73.8	10.3				
D2	61.8			4	13.2	21	
R3	37.4	17.7	1.7	1.8	18.3	23.1	

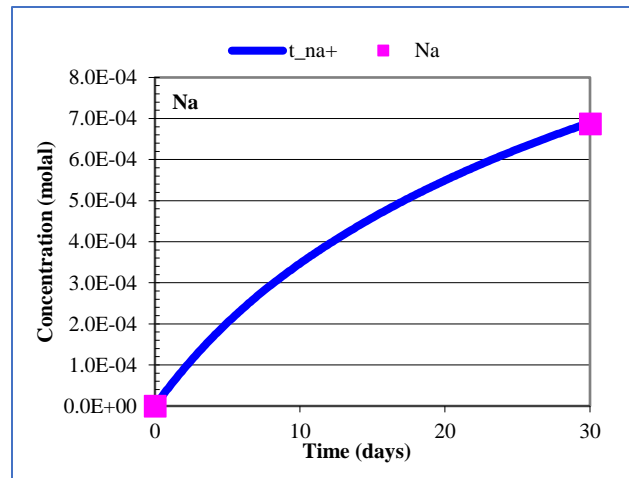
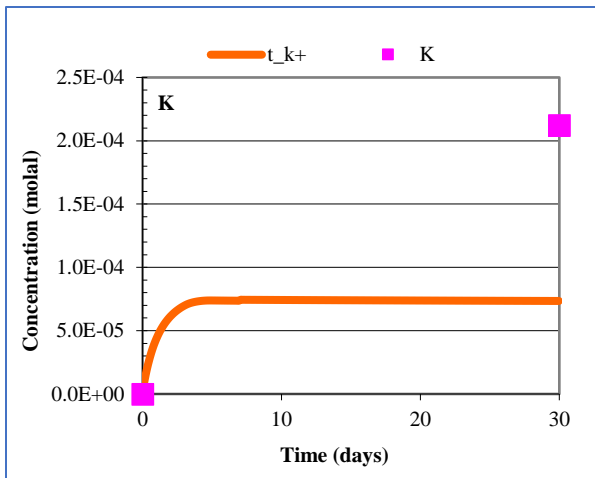
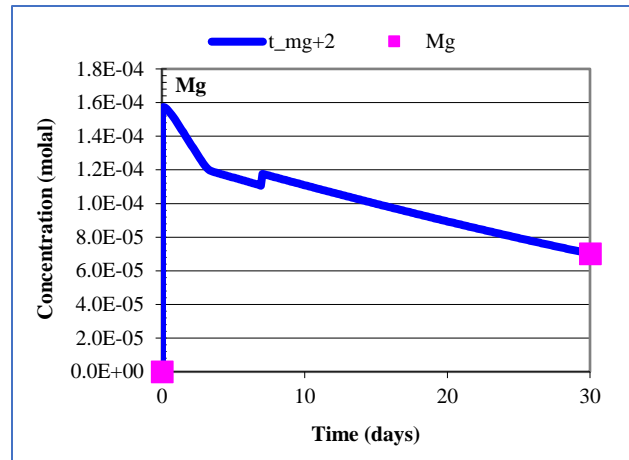
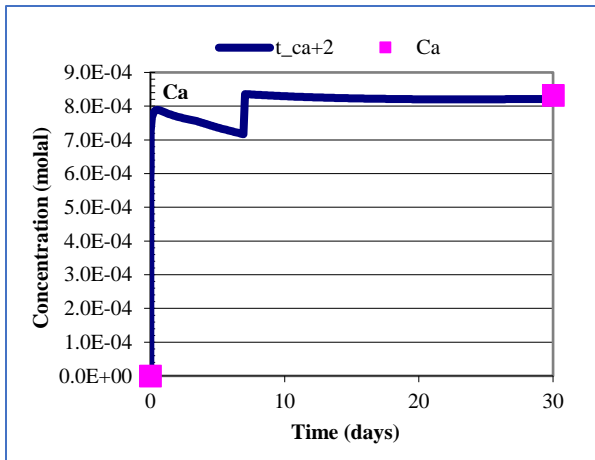
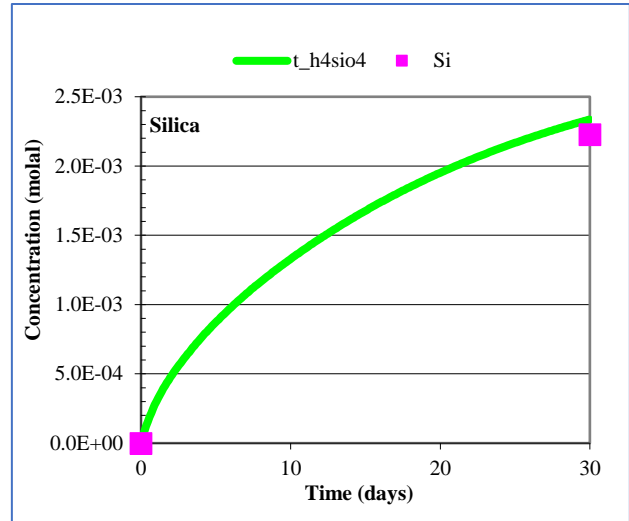
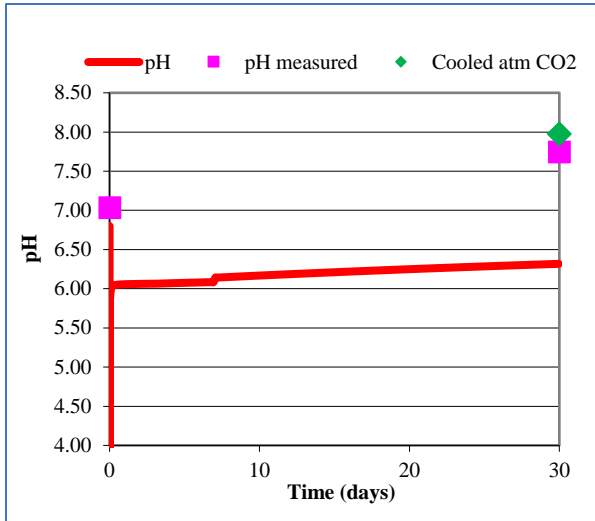
Table A.2: Mineralogical composition (in weight percent) of rock powder samples after 7-days reaction with produced brines.

Mineralogy (7-days Reaction)							
Sample	Quartz (%)	Calcite (%)	Dolomite (%)	Pyrite (%)	Albite (%)	Illite (%)	Andradite (%)
R1	58.6	6.6				34.8	
D1	35.6	5.6			2.1	56.6	
R2	13.4	73.7	12.8				
D2	49.2				14.8	28.7	7.3
R3	28.4	14.2			17.1	40.2	
D1 DI	55.8	5.5			3	35.7	
Remarks: The extension 'DI' means sample was reacted with Deionized water							

Table A.3: Mineralogical composition (in weight percent) of rock powder samples after 7-days reaction with produced brines.

Mineralogy (30-days Reaction)							
Sample	Quartz (%)	Calcite (%)	Dolomite (%)	Pyrite (%)	Albite (%)	Illite (%)	Ankerite (%)
R1	97.4	2.6					
D1	61.8	3.3				35	
R2	39.9	23	17.5				19.6
D2	52.8					47.2	
R3	62.5	7.8				29.7	
R3 DI	56	6.6			20.3	17	
Remarks: The extension 'DI' means sample was reacted with Deionized water							

Appendix B



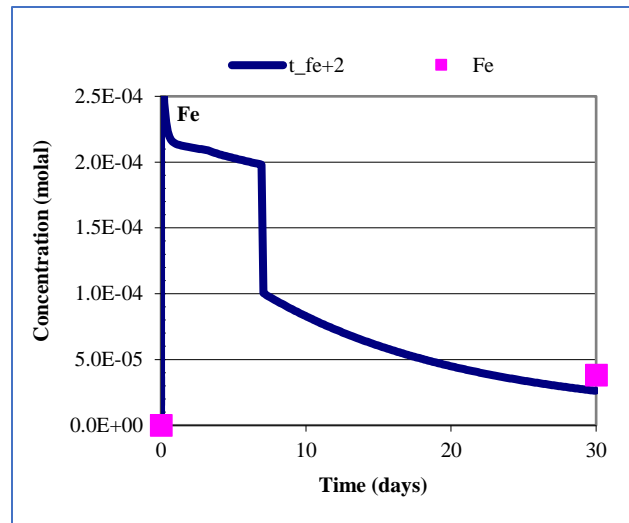
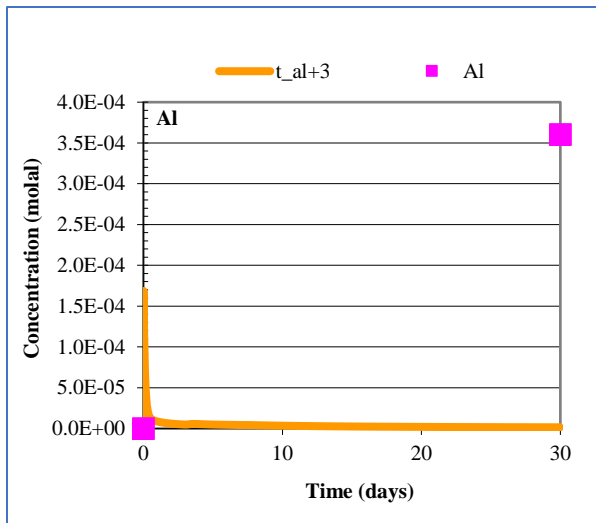


Fig. B Graphs of modeled (lines) and measured (squares) solution compositions based on simulation with DI water. On the pH graph, the final modeled pH (at 95°C) was numerically cooled to 25°C (diamond symbols) for comparison with the measurements.